UNIVERSITÀ
DI PAVIA

Dipartimento di Biologia e Biotecnologie
"Lazzaro Spallanzani"

Laurea Magistralis in Molecular Biology and Genetics

Extracellular vesicles miRNome analysis and long-term culture characterization of mammalian cumulus cells

Supervisor:
Prof. Paola Rebuzzini

Co-supervisor:
Dott. Giulia Brazzale

Experimental thesis by
Carlotta Aldeghi

Academic Year 2025/2026

UNIVERSITÀ
DI PAVIA

Dipartimento di Biologia e Biotecnologie
"Lazzaro Spallanzani"

Laurea Magistralis in Molecular Biology and Genetics

Extracellular vesicles miRNome analysis and long-term culture characterization of mammalian cumulus cells

Analisi del miRNoma di vescicole extracellulari e caratterizzazione di una coltura a lungo termine di cellule del cumulo di mammifero

Supervisor:
Prof. Paola Rebuzzini

Co-supervisor:
Dott. Giulia Brazzale

Experimental thesis by
Carlotta Aldeghi

Academic Year 2025/2026

Abstract

The ovary is the primary female reproductive organ, responsible for both folliculogenesis, development and maturation of ovarian follicles, and secretion of sex hormones. Within antral and Graafian follicles, granulosa cells differentiate into a specialized somatic subpopulation, known as cumulus cells (CCs), which closely envelop the oocyte to form the cumulus-oocyte complex (COC). *In vivo*, CCs maintain direct metabolic and physical contact with the female gamete, playing an indispensable role in supporting its metabolism, modulating meiotic arrest and resumption, and enabling the acquisition of developmental competence. CCs have been successfully isolated and cultured *in vitro* for few days, enabling their use both as a non-invasive marker of oocyte quality and as a feeder layer capable of releasing extracellular vesicles containing active factors that enhance oocyte developmental competence. Their quality and molecular signatures have been studied as crucial indicators to predict or even sustain oocyte maturation in Assisted Reproductive Technology (ART) protocols.

As the role of CCs during the folliculogenesis and the maturation of the female gamete has been clearly evidenced, as well as their potential applications *in vitro* to predict oocyte quality or sustain it, the principal objective thesis work was to deepen our understanding of cumulus cell biology, by pursuing a two-fold strategy: 1) identifying predictive molecular biomarkers of embryonic success; and 2) optimizing a standardized long-term *in vitro* cumulus cells culture.

The miRNome profiling of human cumulus cell-derived extracellular vesicles (EVs) was firstly studied. Specifically, a comparative analysis was performed between EVs produced by human CCs, explanded *in vitro* for 3 days, associated with oocytes that successfully progressed to the blastocyst stage after fertilization, and those that failed to reach blastocyst development (BLASTO vs NoBLASTO), identifing a specific panel of differentially expressed miRNAs. Among these latter, 24 miRNAs were found to be actively involved in key signaling pathways specific for meiosis resumption, fertilization, follicle growth, and acquisition of oocyte developmental competence. Furthermore, downstream bioinformatic analysis revealed a significant evolutionary convergence between human and mouse, which share 55 common miRNAs target genes actively controlling cumulus expansion, fertilization, pre-implantation development, and meiotic resumption. This high conservation validates pre-clinical murine models and suggests that CCs could move beyond their role as mere biomarkers to be exploited as an active feeder layer for *in vitro* oocyte maturation (IVM).

Up to date CCs culture is validated in both mouse and human only up to 72 hours, but short-term cultures are insufficient for human clinical applications, where maturation timeframes vary and minimizing biomaterial waste is crucial. Consequently, to break past this 3-day barrier and lay the

foundation for clinical translation, the second part of this work focused on establishing a long-term primary mouse CC culture to evaluate their viability and functional retention over an extended period of up to 24 days. The evaluation of cell quality and lineage identity revealed that the cultured CCs maintained remarkable phenotypic, morphological, and functional stability up to day 18 of culture, preserving a good morphology, physiological rounded shape and cellular uniformity. Conversely, a critical shift toward senescence occurred only by day 24, marked by a significant increase of a cell population exhibiting a decline in LAMIN B1 expression, a senescent marker, cellular flattening, and a significant upregulation of *Ptx3*, strongly confirming its potential role as a senescence inducer. The cumulus expansion markers *Has2* and *Ptx3* underwent an early downregulation at day 8, likely reflecting a cellular adaptation to the *in vitro* monolayer environment.

Overall, this study explores the complex landscape of female gamete maturation, focusing on the crucial role of cumulus cells and their potential clinical implications in sustaining oocyte developmental competence acquisition and, in general, in ART protocols. These findings establish a baseline for future functional validation of CCs or their derivatives as strategies to enhance the quality of less competent gametes.

Riassunto

L'ovaio è l'organo riproduttivo femminile primario, responsabile sia della folliculogenesi (lo sviluppo e la maturazione dei follicoli ovarici) sia della secrezione degli ormoni sessuali. All'interno dei follicoli antrali e di Graaf, le cellule della granulosa si differenziano in una sottopopolazione somatica specializzata, nota come cellule del cumulo (CC), che avvolgono strettamente l'ovocita a formare il complesso cumulo-ovocita (COC). *In vivo*, le CC mantengono un contatto metabolico e fisico diretto con il gamete femminile, svolgendo un ruolo indispensabile nel supportarne il metabolismo, nel modulare l'arresto e la ripresa meiotica e nel consentire l'acquisizione della competenza dello sviluppo. Le CC sono che state isolate e coltivate con successo *in vitro* per pochi giorni, consentendo il loro utilizzo sia come marcatore non invasivo della qualità ovocitaria, sia come feeder layer in grado di rilasciare vescicole extracellulari contenenti fattori attivi che migliorano la competenza dello sviluppo dell'ovocita. La loro qualità e le loro firme molecolari sono state studiate come indicatori cruciali per prevedere o persino sostenere la maturazione ovocitaria nei protocolli di Procreazione Medicalmente Assistita (PMA).

Poiché il ruolo delle CC durante la folliculogenesi e la maturazione del gamete femminile è stato chiaramente evidenziato, così come le loro potenziali applicazioni in vitro per prevederne o sostenerne la qualità, l'obiettivo principale di questo lavoro di tesi è stato quello di approfondire la nostra comprensione della biologia delle cellule del cumulo, perseguendo una duplice strategia: 1) identificare biomarcatori molecolari predittivi del successo embrionale; e 2) ottimizzare una coltura standardizzata a lungo termine in vitro delle cellule del cumulo.

Il profilo del miRNoma delle vescicole extracellulari (EV) derivate da cellule del cumulo umane è stato studiato per primo. Nello specifico, è stata eseguita un'analisi comparativa tra le EV prodotte da CC umane, espanse in vitro per 3 giorni, associate a ovociti che sono progrediti con successo allo stadio di blastocisti dopo la fecondazione, e quelle che non hanno raggiunto lo sviluppo di blastocisti (BLASTO vs NoBLASTO), identificando un pannello specifico di miRNA espressi in modo differenziale. Tra questi ultimi, 24 miRNA sono risultati attivamente coinvolti in vie di segnalazione chiave specifiche per la ripresa della meiosi, la fecondazione, la crescita follicolare e l'acquisizione della competenza dello sviluppo ovocitario. Inoltre, l'analisi bioinformatica a valle ha rivelato una significativa convergenza evolutiva tra uomo e topo, i quali condividono 55 geni bersaglio comuni dei miRNA che controllano attivamente l'espansione del cumulo, la fecondazione, lo sviluppo pre-impianto e la ripresa meiotica. Questa elevata conservazione convalida i modelli murini pre-clinici e suggerisce che le CC potrebbero andare oltre il loro ruolo di semplici biomarcatori per essere sfruttate come feeder layer attivo per la maturazione in vitro dell'ovocita (IVM).

Ad oggi, la coltura delle CC è validata sia nel topo che nell'uomo solo fino a 72 ore, ma le colture a breve termine sono insufficienti per le applicazioni cliniche umane, dove i tempi di maturazione variano e ridurre al minimo lo spreco di materiale biologico è fondamentale. Di conseguenza, per superare questa barriera dei 3 giorni e gettare le basi per la traslazione clinica, la seconda parte di questo lavoro si è concentrata sull'istituire una coltura primaria a lungo termine di CC di topo per valutarne la vitalità e il mantenimento funzionale su un periodo esteso fino a 24 giorni. La valutazione della qualità cellulare e dell'identità di lignaggio ha rivelato che le CC coltivate hanno mantenuto una notevole stabilità fenotipica, morfologica e funzionale fino al giorno 18 di coltura, preservando una buona morfologia, una forma arrotondata fisiologica e un'uniformità cellulare. Al contrario, un passaggio critico verso la senescenza si è verificato solo entro il giorno 24, contrassegnato da un aumento significativo di una popolazione cellulare che mostrava un calo dell'espressione di LAMIN B1, un marcatore di senescenza, dall'appiattimento cellulare e da una significativa upregulation di Ptx3, confermando fortemente il suo potenziale ruolo come induttore di senescenza. I marcatori di espansione del cumulo Has2 e Ptx3 hanno subito una precoce downregulation al giorno 8, riflettendo probabilmente un adattamento cellulare all'ambiente del monolayer in vitro.

Nel complesso, questo studio esplora il complesso panorama della maturazione del gamete femminile, concentrandosi sul ruolo cruciale delle cellule del cumulo e sulle loro potenziali implicazioni cliniche nel sostenere l'acquisizione della competenza dello sviluppo ovocitario e, in generale, nei protocolli di PMA. Questi risultati stabiliscono una linea di base per la futura validazione funzionale delle CC o dei loro derivati come strategie per migliorare la qualità dei gameti meno competenti.

Index

1. Introduction

1.1 The ovary and the folliculogenesis

1.1.1 Anatomy of the ovary and its physiological functions

The ovary is structurally organized into two distinct regions, the inner medulla and outer cortex [**Figure 1**]**.** The medulla occupies the central portion of the organ and contains loose connective tissue, together with blood and lymphatic vessels, and nerves, that enter through the hilum. The rich vascular network of the medulla plays a critical role in supporting the cyclical metabolic demands of the organ, particularly during follicular growth and corpus luteum formation. The outer cortex, in contrast, is densely populated by ovarian follicles at various stages of development, embedded within a highly cellular stromal connective tissue, predominantly composed of spindle-shaped fibroblast-like cells. As these follicles develop, they migrate toward the deeper layers of the stroma before returning to the cortical surface during the final stages of folliculogenesis (Ross & Pawlina, 2010).
The outermost layer of the cortex is covered by a simple squamous-to-cuboidal epithelium, the surface epithelium, which is continuous with the peritoneum and plays a role in ovulation and post-ovulatory repair.

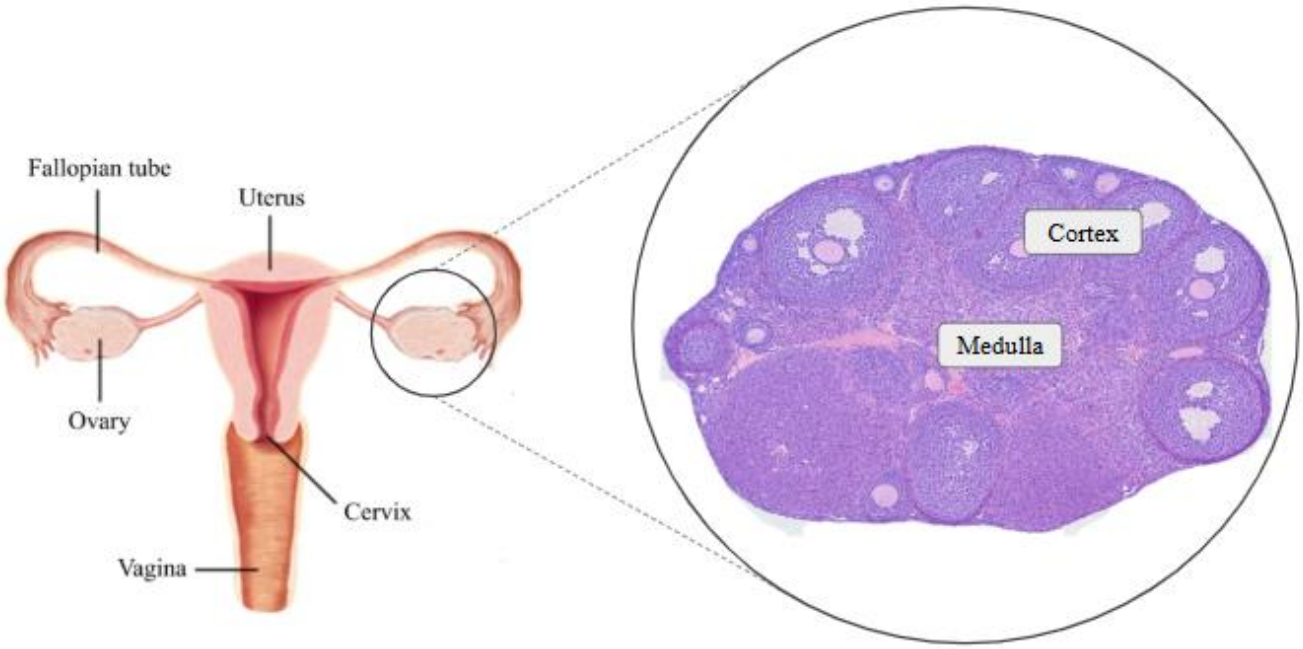

Figure 1 Anatomical view of the female reproductive tract (left) with histological detail of ovarian cortex and medulla (right). Ovary section from the Laboratory of Biology and Biotechnology of Reproduction of the University of Pavia, and image adapted from Encyclopaedia Britannica

The mammalian ovary has two main functions: the secretion of sex steroid hormones, that support itself and other tissues, and the generation of developmentally competent oocytes (Pietroforte et al., 2025). With regard to its endocrine function, the ovary produces estrogens, progesterone, and androgens in a cyclically regulated manner, primarily through the coordinated activity of theca cells (TCs) and granulosa cells (GCs) of the developing follicle, as well as through the corpus luteum following ovulation. These hormones drive wide-ranging effects not only on the reproductive tract, but also on bone metabolism, the cardiovascular system, and the central nervous system (Nilsson et al., 2001). With regard to its gametogenic function, the ovary maintains the female germline throughout reproductive life, governing the progressive maturation of oocytes within their follicular units (Pietroforte et al., 2025). This dual role, endocrine and gametogenic is tightly coordinated through a complex interaction of gonadotropic hormones, local paracrine signals, and intra-follicular communication, whose dynamics are further discussed in detail.

1.1.2 Folliculogenesis

Folliculogenesis is the process by which female germ cell develops with the somatic cells of the ovary for the maturation of fertilizable eggs. This process lasts one year in the human and twenty-five days in the mouse (Zeleznik et al., 2015).

The functional unit formed by germ and somatic cells is called follicle. Its development is highly dynamic and dependent to different signals according to the steps of maturation: early folliculogenesis is driven by signals within the ovary, while endocrine hormones from the pituitary gland are necessary for folliculogenesis to proceed afterwards. Nevertheless, the ovary itself has an active role, it produces feedback and feedforward hormones that regulate hypothalamic and pituitary function. In addition, a continuous bidirectional crosstalk between the oocyte and the somatic-derived cells contributes to the normal follicle development (Zeleznik & Stouffer, 2015).

Folliculogenesis is characterized by morphological and cytological changes of all cellular components of the follicle, due to the meiotic progression of the oocyte and the structural reorganization of the surrounding somatic cells (Erickson, 2008). Based on these evidences, Pedersen and Peters proposed a classification, commonly used for mice, based on oocyte size, GC numbers, and follicular morphology. According to the classification proposed by Pedersen and Peters in 1968 (Pedersen & Peters, 1968), follicular development is categorized into eight distinct stages. Within this framework, small follicles encompass types 1 to 3a, medium follicles range from 3b to 5a, and large follicles include types 5b through 8 (Pedersen & Peters, 1968) [**Figure 2**].

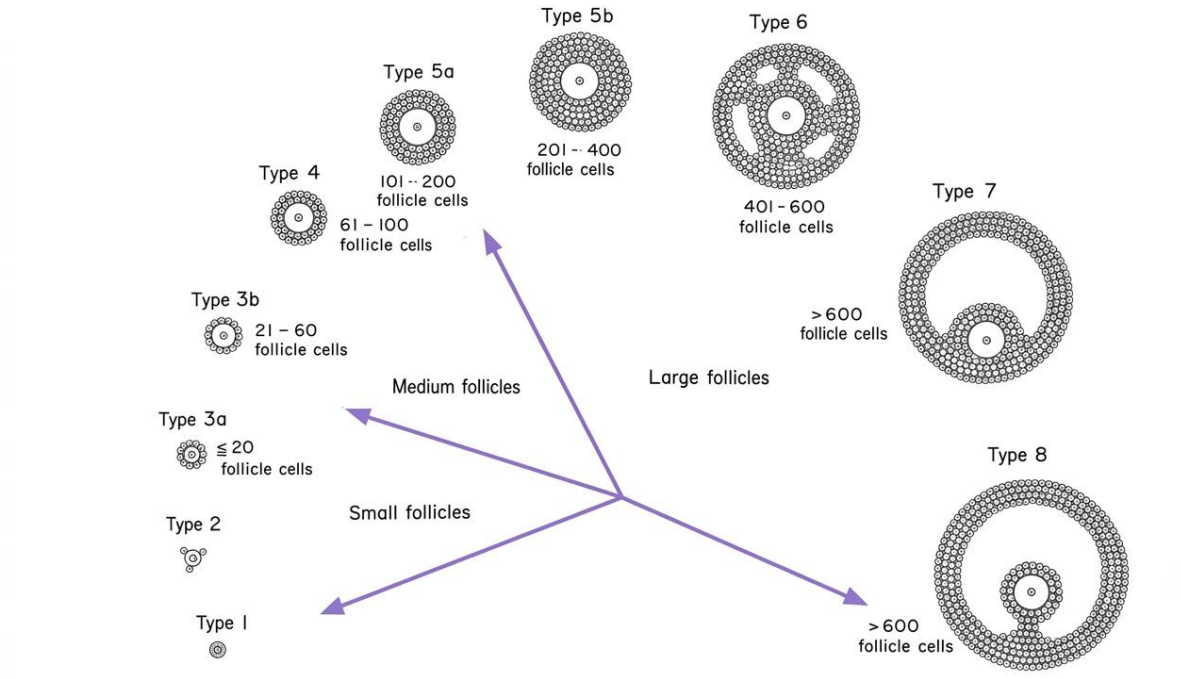

Figure 2 Pedersen & Peters' follicle classification (adapted from Pedersen & Peters, 1968)

For broader descriptive purposes, follicles are more commonly classified based on their morphological features as primordial, primary, secondary (also known as preantral), antral, and Graafian follicles (Pangas & Rajkovic, 2015) [**Figure 3**].

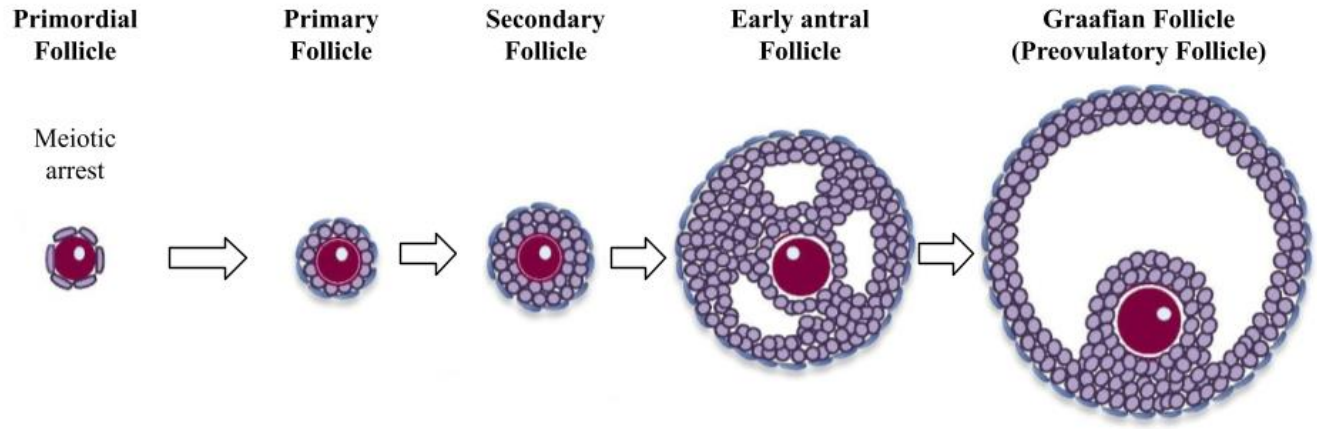

Figure 3 Canonical classification (adapted from Sanchez & Smitz, 2012)

Oocyte meiotic maturation is tightly coupled to follicular development, oocytes enter meiosis during embryonic life, starting between the 11th and 12th week of gestation in humans and at embryonic day 13.5 (E13.5) in mice. At birth, the entire pool of oocytes is arrested in the diplotene stage of prophase I. At this phase, the oocyte is characterized by the presence of a large, distinct nucleus called Germinal Vesicle (GV). Following puberty in human and approximately after 3 weeks postnatal in mice, meiosis resumes shortly before ovulation in response to the luteinizing hormone (LH) surge, leading to Germinal Vesicle Breakdown (GVBD); however, it reaches a second arrest at metaphase II. The completion of the second meiotic division occurs only upon fertilization; otherwise, the oocyte remains arrested and eventually undergoes degeneration (Pangas & Rajkovic, 2015).

In parallel with oocyte meiotic maturation, significant morphological changes occur within the entire follicle. These transformations drive the differentiation of somatic cells and the acquisition of specific functional properties, which ultimately determine the developmental competence and physiological state of the follicle (Eppig, 2001).

1.1.3 From primordial to primary follicles

Primordial follicles consist of a primary oocyte, approximately of 25 µm in diameter, arrested in diplotene of meiosis I, and a single layer of flattened GCs, which are delimited from the surrounding ovarian stroma by a basal lamina [**Figure 4**] (Erickson, 2008). This initial organization, by regulating cellular communication and limiting direct exposure to the systemic blood supply, maintains oocyte in a dormant state, preventing its exposure of premature environmental stimuli (Zhang & Liu, 2015).

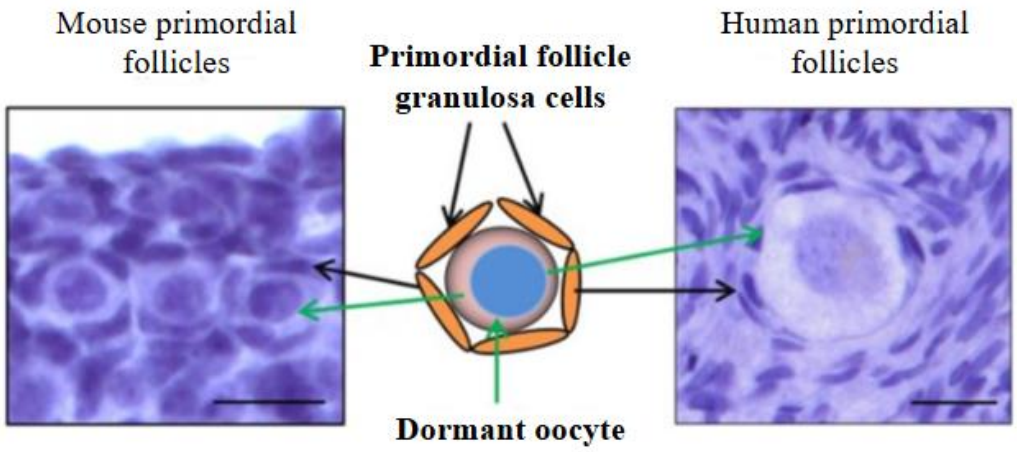

Figure 4 Primordial follicle organization (Zhang & Liu, 2015).

The entire pool of primordial follicles presents at birth (approximately 400,000 in humans and 10,000 in mice) constitutes the total reservoir of germ cells available during the entire female's reproductive lifespan. The recruitment process, which involves a daily cohort of follicles, estimated at 30–50 in young humans (Gougeon, 1996) and roughly 100–150 in mice (Pedersen, 1970), initiates shortly after follicle formation and continues until the pool is depleted at menopause. This transition, known as initial recruitment, is mediated by local autocrine and paracrine signalling within the ovarian microenvironment. In the oocyte, the PTEN/PI3K signalling pathways is a crucial regulator of primordial follicle activation, acting as a molecular switch for follicular recruitment (Sanchez & Smitz, 2012). In addition, the interaction between KIT ligand and its receptor, early expressed respectively by somatic cells and oocyte, controls initial follicular growth by promoting TCs recruitment, proliferation of GCs and stimulating oocyte growth. The overall rate of recruitment is further modulated by the Anti-Müllerian Hormone (AMH), secreted by the GCs of growing follicles, which acts as a paracrine inhibitory signal that limits the initial recruitment of primordial follicles. By regulating the ratio between quiescent and activated follicles, AMH ensures that follicular depletion is spread across the female's reproductive lifespan (Sanchez & Smitz, 2012).

The first morphological indicator of this process is the transition of GCs from a flat to a cuboidal phenotype. Following this shift, GCs initiate DNA synthesis and enter the mitotic cycle, albeit at a low initial rate (Erickson, 2008). At this stage, this follicle becomes a primary follicle, constituted by a single layer of one or more cuboidal GCs surrounding the oocyte [**Figure 5a**]. Parallel to the morphological changes, these cells start to express follicle-stimulating hormone (FSH) receptors. On the other hand, the oocyte starts transcriptional activation, increasing the level of RNA synthesis of a huge number of fundamental genes. For instance, one of these is the transcription and expression of genes encoding the zona pellucida proteins (i.e. ZP-1, ZP-2 and ZP-3). Polymerization of these proteins will form a glycoprotein envelope around the oocyte which has a role in fertilization, ZP-3 is the species-specific sperm-binding molecule, and protects and supports embryo development till blastocyst. In addition, cytoplasmatic protrusions of GCs, called trans zonal projections, start to extend across the membrane and take contact with the oocyte forming junctions [**Figure 5b**]. These junctions provide the flow of ions, metabolites and other low-molecular-weight signalling molecules, establishing a continuous bidirectional communication that drives follicle maturation and acquisition of oocyte competence (Cavalcanti et al., 2023). In this respect, a primary follicle matures in secondary follicle and the maturation is mainly driven by intraovarian paracrine factors produces by the oocytes and the surrounding GCs, rather than FSH perturbation, nevertheless the presence of FSH receptors (Sanchez & Smitz, 2012).

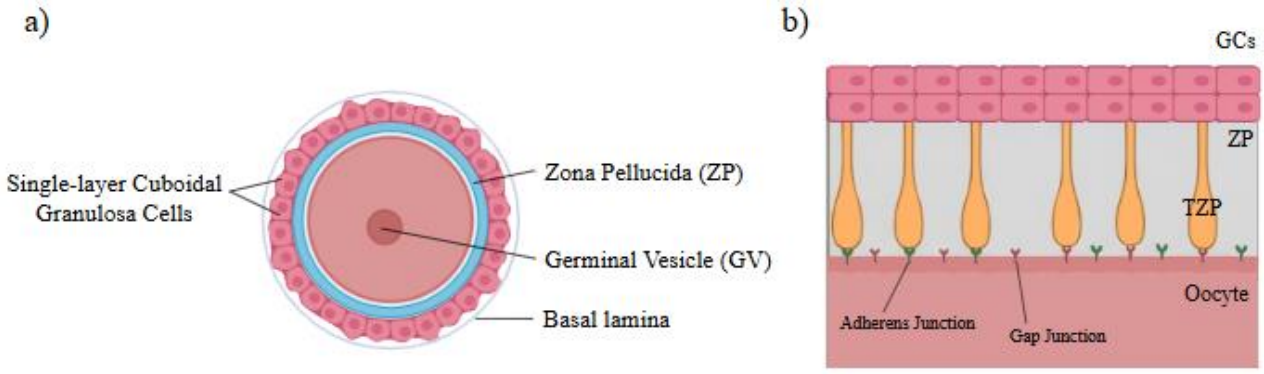

Figure 5 a) Structural organization of the primary follicle; b) Representation of transzonal projections (TZPs) and intercellular communication between granulosa cells (GCs) and the oocyte through gap and adherens junctions (created in BioRender)

1.1.4 Secondary follicle

A secondary follicle is a preantral follicle that develops through the proliferation of GCs, which form multiple layers of cuboidal or low columnar cells around the oocyte. This massive proliferation may be imputed by growth differentiation factor-9 (GDF-9), highly expressed in the ovary. In addition, during this stage of maturation, stroma-like cells, around the basal lamina, start to differentiate forming theca layer which will be differentiated further in inner theca interna (TI) and outer theca externa (TE). At the same time, between TCs, the angiogenesis process starts, bringing to the formation of small vessels. This signs the stage at which the follicle becomes dependent on hormones (e.g. FSH, LH) and on nutrients circulating in the blood stream. In turn, the follicle takes advantage of the blood stream to release waste and secretory products. In the TI, cells are responsible to the production of androgenic steroids, androstenedione and testosterone, in response to LH (Cavalcanti et al., 2023). Moreover, at this stage all GCs express FSH receptors (Erickson, 2008).

In mice, once the secondary follicle reaches a diameter of approximately 200 µm, the oocyte attains its maximum size (80–100 µm); nevertheless, the follicle continues to expand until reaching a final diameter of roughly 600 µm (Griffin et al., 2006). This disparity highlights that subsequent follicular growth is driven primarily by the proliferation and differentiation of somatic cells. Their complex structural reorganization and evolving signalling profile are essential to regulate the final stages of oocyte maturation. Crucially, while the oocyte has ceased its physical expansion, it remains metabolically active, accumulating the transcripts and organelles necessary for future embryonic development. This process is governed by a continuous bidirectional communication loop between the germ cell and the surrounding somatic compartment, which ultimately determines the acquisition of developmental competence (Eppig, 2001; Gilchrist et al., 2008).

1.1.5 From pre-antral to antral follicle

By the conclusion of the maturation in secondary (preantral) follicle, it is characterized by distinct structural components: a fully grown oocyte enclosed within the ZP, six to nine layers of proliferating GCs, a basal lamina, and the differentiated TI and TE layers. The transition toward the antral stage initiates with cavitation, a process in which small, fluid-filled spaces begin to join together among the GCs controlled by autocrine and paracrine mechanisms (Erickson, 2008). As the volume of this follicular fluid increases, these spaces create a single large cavity known as the antrum. This expansion progressively moves the oocyte to one pole of the follicle [**Figure 6**].

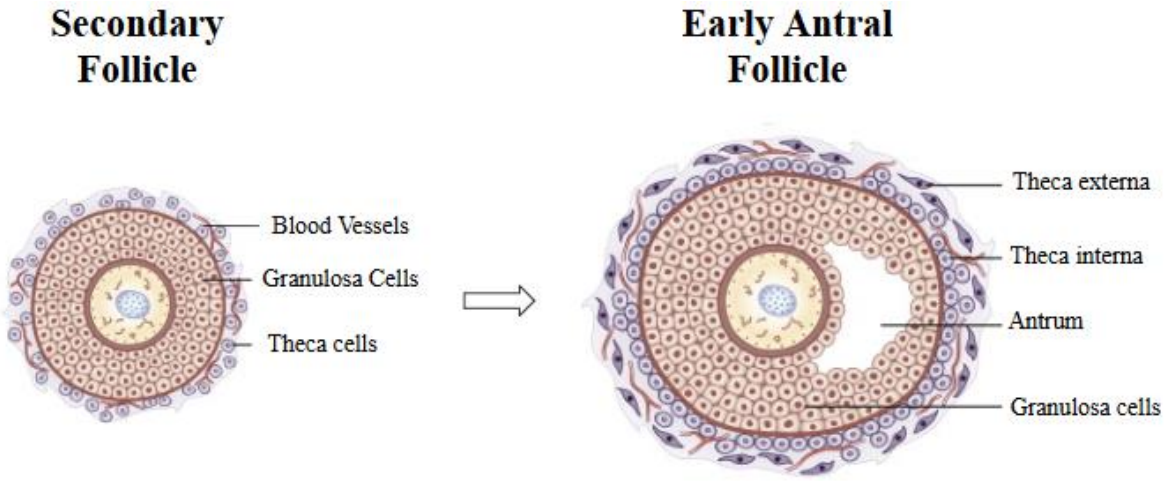

Figure 6 Morphological changes between Secondary Follicle and Early Antral Follicle (Anthony W. et al, 2015)

The progression from the preantral to the antral stage is governed by a sophisticated network of growth factors, hormones, and physical intercellular connections. Central to this process is the bidirectional dialogue between the germ cell and its somatic support, primarily driven by members of the TGF-beta superfamily. The oocyte-secreted factors GDF9 and BMP15 act in potent synergy to stimulate GC proliferation and survival; specifically, GDF9 promotes the expression of FSH receptors and activates the PI3K/AKT pathway to prevent apoptosis, while BMP15 drives mitosis. This growth-oriented environment is further modulated by the shifting balance between activins and inhibins: while Activin-A acts as a powerful mitogen in the early stages, its influence gradually declines as Inhibin-A and Inhibin-B levels rise, driving the shift toward follicle selection and antrum formation. In addition to these paracrine signals, the transition is fine-tuned by systemic and local hormonal regulators. Androgens enhance the proliferation and survival of preantral follicles through the androgen receptor (AR), providing a foundational stimulus for growth. However, biochemical signalling alone is insufficient without the structural synchronization provided by gap junction

proteins. Communication between individual GCs is maintained by Connexin 43 (Cx43), while the vital link between the oocyte and the granulosa layer is mediated by Connexin 37 (Cx37). Thus, the successful acquisition of an antral cavity is the result of a delicate equilibrium where oocyte-derived proliferative signals, hormonal feedback loops, and direct cytoplasmic communication converge to determine follicular fate (Sanchez & Smitz, 2012). In monovulatory species, this process culminates in the maturation of a single dominant follicle while the remaining follicles undergo atresia. Conversely, in polyovulatory species, several follicles reach the final mature state, becoming ready for being ovulated (Webb et al., 2003).

1.1.6 Graafian follicle

At the end of this structural reorganization, the follicle reaches its final mature stage, referred to as the Graafian follicle, namely pre-ovulatory follicle. All the large follicles, which present a cavity, are classified into the heterogenous family of graafian follicle. They may differ in size but the basic structure is maintained. It is based on the presence of six distinct histologic components: TI and TE, basal lamina, GCs, oocyte, and antrum filled with follicular fluid [**Figure 7**].

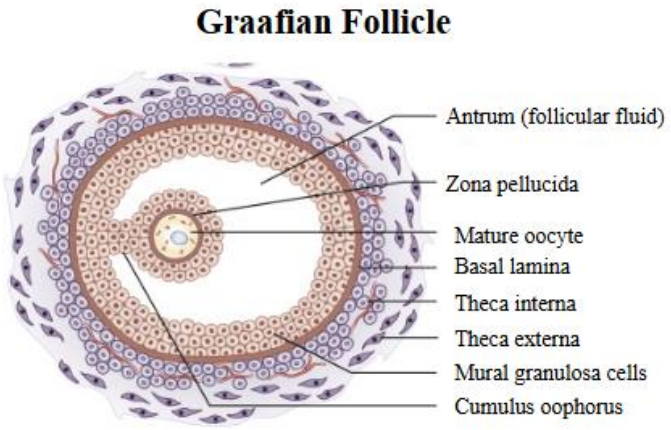

Figure 7 Graafian Follicle organization

The TE is composed of smooth muscle cells which are innervated by autonomic nerves and play a role during ovulation and atresia. The TI is made of theca interstitial cells (TICs) nestled within a matrix of loose connective tissue and blood vessels (Erickson, 2008). The GCs differentiate into two main populations: mural granulosa cells (MGCs), which are part of the follicular wall and cumulus cells (CCs), which surround the oocyte; the latter are further organized into the cumulus oophorus, which links the mural and the cumulus compartment, and the corona radiata which is in close

proximity with the oocyte (Eppig, 2001). From a histological point of view the mural compartment is composed of a pseudostratified epithelium of tall columnar GCs, all anchored at the basal lamina (Erickson, 2008); moreover, these two populations may be distinguished at molecular level. For example, GCs express LH receptors at different levels, with a high expression in MGCs, especially those in close proximity to the basal lamina. The establishment of this heterogeneous pattern is primarily driven by the oocyte through the secretion of paracrine factors, such as GDF9 and BMP15, which establish a specific bidirectional metabolic coupling. Unlike mural cells, CCs exhibit a specialized transcriptomic profile dedicated to supporting oocyte energy metabolism and protecting the germ cell from oxidative stress.

Furthermore, in response to the pre-ovulatory LH surge, the CCs undergo a critical process known as cumulus expansion. This involves the synthesis of a hyaluronic acid-rich extracellular matrix, a structural remodelling essential for oocyte meiotic maturation, follicular rupture, and subsequent fertilization. Ultimately, this complex structural and functional specialization prepares the Cumulus-Oocyte Complex (COC) for its final destiny: the LH-triggered ovulation and the acquisition of full developmental competence (Eppig, 2001).

1.2 Somatic components of the ovarian follicle

The development of a high-quality oocyte during folliculogenesis does not depend solely on the oocyte itself, but relies on the follicular somatic cells as already introduced before. These cells are anatomically and functionally distinct, but together they establish a coordinated microenvironment that builds the structural, endocrine, and metabolic requirements of the maturing oocyte (Gilchrist et al., 2008).

Within the follicle, the somatic compartment is composed of two primary cell lineages: the TCs and the GCs. While both lineages are essential, they differ considerably in their roles. Theca cells, organized in the TI and TE layers, serve partially structural and partially endocrine functions. The TI is a highly vascularized layer of differentiated steroidogenic cells, characterized by numerous mitochondria, abundant agranular endoplasmic reticulum, and lipid vesicles, all hallmarks of steroid-secreting cells. Through the action of key enzymes such as Cytochrome P450 (CYP11A), these cells produce androgens that serve as precursors for estrogen synthesis (Magoffin, 2005). In contrast, the TE is a less organized, non-steroidogenic layer with a predominantly structural and contractile function (Magoffin, 2005; Erickson, 2008).

Separated from the theca layer by the basal lamina, the GCs represent the somatic cells most closely associated with the oocyte. Avascular until the secondary follicle stage, they rely on diffusion for nutrient and signal exchange. As folliculogenesis progresses, GCs undergo functional differentiation into two distinct subpopulations: MGCs and CCs (Eppig, 2001) [**Figure 7**]. MGCs are highly responsive to gonadotropins and are primarily responsible for converting theca-derived androgens into estrogens, as well as expressing LH receptors required for ovulation. CCs, on the other hand, maintain direct physical and metabolic contact with the oocyte, actively supporting its metabolism and regulating meiotic arrest and resumption (Eppig, 2001; Wigglesworth et al., 2013).

Therefore, among all somatic cell types, CCs occupy a uniquely privileged position: their close association with the oocyte makes them not merely supportive, but indispensable for the acquisition of oocyte developmental competence. Their specific roles and molecular functions will be discussed in detail in the following paragraphs.

1.2.1 The role of CCs in acquisition of oocyte developmental competence

The acquisition of oocyte developmental competence, defined as the capacity of the female gamete to complete meiosis, support fertilization, and sustain early embryonic development up to implantation, is not a property conferred at the time of the LH surge, but is progressively built throughout folliculogenesis through a series of coordinated molecular events in which cumulus-derived signals play a central role (Coticchio et al., 2015; Dumesic et al., 2015). This process unfolds according to the architecture of the COC, whose structural base is made by TZPs, which represent the direct contact with the oolemma, serving as channels for gap junctional exchange of ions, cAMP, cGMP, amino acids, and metabolic intermediates (Li & Albertini, 2013). The number of TZPs increases progressively with oocyte growth, in response to oocyte-secreted GDF9 and BMP15, reflecting the escalating demand for somatic support as the oocyte enlarges (Monniaux, 2016). This represents one of the clearest examples of how, rather than being a passive recipient of somatic support, the oocyte itself actively orchestrates the behaviour of its surrounding CCs through oocyte-secreted factors (OSFs), establishing a true functional interdependence that lies at the heart of competence acquisition [**Figure 8**].

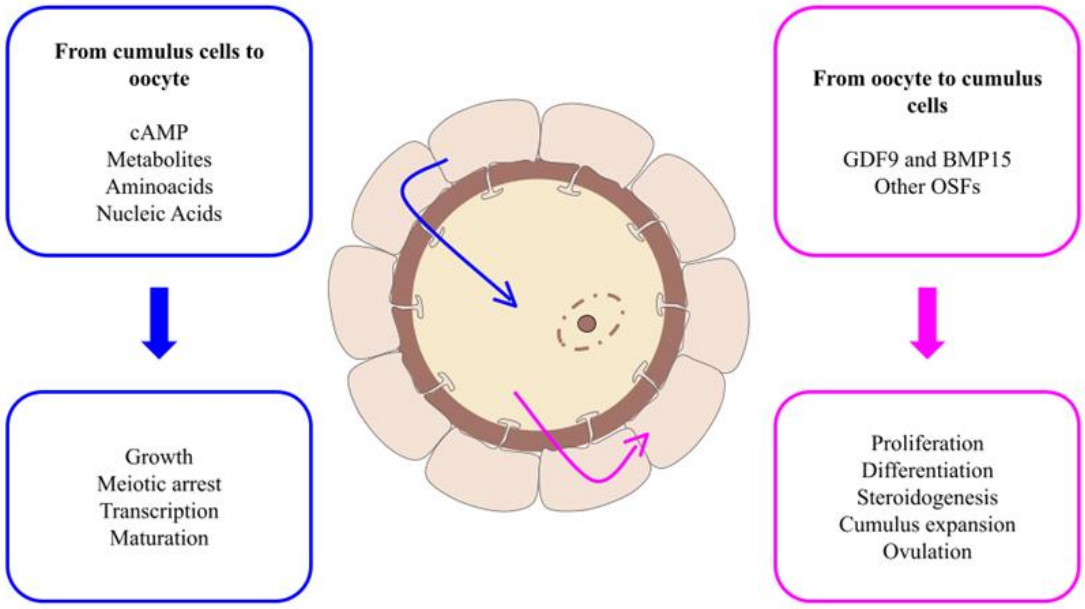

Figure 8 Bidirectional molecular communication within the COC and its functional effects

A particularly well-characterized axis of this support is the metabolic cooperation between CCs and the oocyte. The oocyte is inherently deficient in several key enzymatic pathways: it is unable to carry out effective glycolysis, cholesterol biosynthesis, or direct amino acid uptake [**Figure 9**]. To compensate, it relies entirely on CCs to perform these functions on its behalf. GDF9 and BMP15, secreted by the oocyte itself, directly reprogram CCs metabolism by upregulating glycolytic flux, promoting the pentose phosphate pathway (PPP), and enhancing the synthesis and transfer of metabolic substrates, primarily pyruvate, that regulate oocyte oxidative phosphorylation (Gilchrist et al., 2008; Su et al., 2009). In this regard, the oocyte's ability to metabolize glucose via glycolysis is limited due to the lack of expression of the high-affinity insulin-regulated glucose transporter SLC2A4 (GLUT4) and the low activity of phosphofructokinase (PFK), a rate-limiting glycolytic enzyme. Low glycolytic activity leads to poor oocyte developmental competence, whereas high glycolytic activity has been associated with increased blastocyst development. An important alternative metabolic route is the PPP, which produces NADPH and ribose 5-phosphate (R5P). It is generally admitted that augmented PPP activity within the CCs leads to a meiosis-inducing signal that acts on the oocyte to induce GVB (Martinez et al., 2023). Beyond glucose metabolism, CCs provide cholesterol precursors essential for sustaining early preimplantation embryo development, and mediate amino acid uptake through the overexpression of the transporter SLC38A1, thereby supporting oocyte cytoplasmic maturation (Ezz & Balboula, 2026). The efficiency of this metabolic

axis has been directly correlated with oocyte quality: CCs surrounding developmentally competent oocytes display a distinct metabolic signature, characterized by higher glycolytic activity and more efficient mitochondrial coupling, compared to those associated with oocytes of poor developmental potential (Sutton-McDowall et al., 2010; Feuerstein et al., 2007).

Alongside their metabolic role, CCs play a pivotal function in protecting the oocyte from oxidative damage [**Figure 9**]. During the main metabolic pathways occurring within the oocyte, reactive oxygen species (ROS) are inevitably generated as by-products, and their accumulation can compromise organelle integrity and DNA stability, ultimately impairing developmental competence. The oocyte has a low ability to mobilize sufficient antioxidant defence on its own. Thus, CC antioxidants are the main responsible for the oocyte oxidative stress defence. CCs act as the primary source of antioxidant defence by supplying reduced glutathione (GSH), with key roles in biomolecular protection against oxidative damage and detoxification processes, and of NADPH, which reduces GSSG to GSH [**Figure 9**]. Although GSH is also produced by the oocyte, optimal GSH levels are dependent on CCs synthesis. Furthermore, catalase (CAT) is an antioxidant enzyme

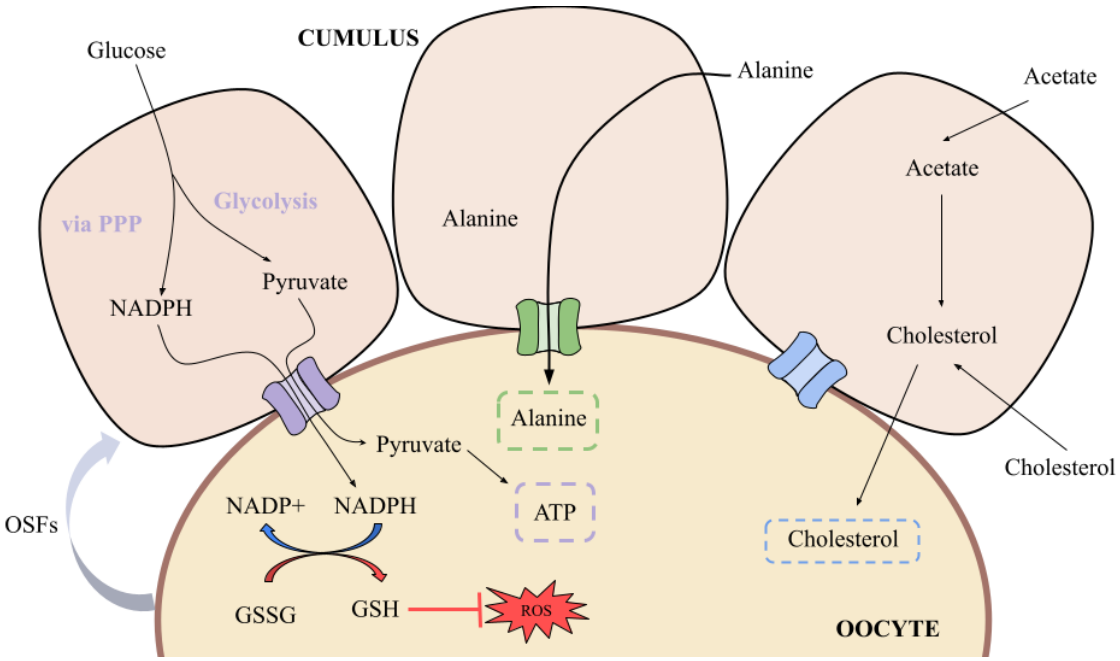

Figure 9 Metabolic cooperation between cumulus cells and the oocyte (adapted from Richani et al., 2021)

low expressed in oocytes but highly produced by CCs, metabolizing H_2O_2 into non-reactive molecules and protecting the oocyte from oxidative stress damage. Glutathione-S-transferases (GSTs) are also an antioxidant enzyme family produced by CCs to protect oocytes from oxidative damage and lipid peroxidation caused by ROS and toxic compounds, using GSH as a cofactor. Superoxide dismutase (SOD), catalyzing the metabolization of the reactive superoxide anion into H_2O_2 and O_2, is expressed

in both CCs and oocytes. Its expression and activity level in CCs was positively correlated with successful pregnancy rates (Martinez et al., 2023; Ezz & Balboula, 2026).

CCs also contribute to the regulation of the oocyte's epigenetic landscape, a dimension of competence acquisition that is increasingly recognized as fundamental cumulus-derived signals actively participate in orchestrating these epigenetic transitions, linking the functional state of the somatic compartment to the nuclear maturation of the oocyte (Zuccotti et al., 1995; De La Fuente, 2006).

An additional and increasingly recognized layer of CCs-oocyte communication is provided by extracellular vesicle (EVs). The latter are membrane-enclosed vesicles of cellular origin that carry a large array of active molecules, including lipids, proteins, and nucleic acids. They are present in the follicular fluid and may reach the oocyte by direct endocytosis. Growing evidence indicates that CCs secrete EVs containing substances that influence both their own function and the oocyte: for instance, CCs expansion is promoted in the presence of EVs in the bovine and equine species through the actions of their cargo (Martinez et al., 2023).

Among the diverse molecular cargos carried by EVs, miRNAs have attracted considerable interest for their role in post-transcriptional gene regulation, contributing to the modulation of key pathways involved in follicle growth, follicular dominance or atresia, and the acquisition of oocyte developmental competence (Fiorentino et al., 2024; Voros et al., 2025). Notably, miRNAs encapsulated in EVs facilitate paracrine communication among GCs, CCs, and the oocyte, regulating processes including apoptosis, glycolysis, mitochondrial function, and cell cycle progression. In this regard, miR-132, miR-212, and miR-214 released from EVs have been shown to trigger oocyte meiosis resumption by negatively regulating genes encoded for follicle maturation-inhibiting factors (Martinez et al., 2023). More broadly, miRNA profiles of intrafollicular exosomes have been shown to target pathways such as ubiquitin-mediated signalling modulating meiotic resumption, WNT signalling during follicular development and luteinization, MAPK signalling facilitating GC proliferation and cumulus expansion, and TGF-β family members exerting permissive effects on MAPK signalling activation in CCs (Fiorentino et al., 2024; Voros et al., 2025; Zhao et al., 2025)

Beyond their metabolic, antioxidant, epigenetic, and paracrine roles, CCs are also the primary regulators of meiotic arrest and its timely resumption. Throughout most of folliculogenesis, the oocyte is maintained in arrest at the diplotene stage of prophase I by elevated intraoocyte cAMP levels, till ovulation. In order to control the correct timing of meiotic resumption different factors interact with each other. First, an elevate concentration of cyclic adenosine monophosphate (cAMP) in oocyte is needed to maintain meiotic arrest; therefore, when ovulation is occurring, LH activates cAMP phosphodiesterase (PDE3A) which will decrease cAMP concentration. The early meiosis activation

is avoided by the influx of cyclic guanosine monophosphate (cGMP) from the CCs, via gap junctions, which will inhibit PDE3A activity. cGMP is produced from GTP in GCs by guanylyl cyclases, mainly natriuretic peptide receptor 2 (NPR2). GTP itself is originated from inosine monophosphate (IMP), derived from the convergence of the de novo purine metabolic pathway and the HPRT salvage pathway, which avoid hypoxanthine (HX) demolition and excretion, after several enzymatic reaction, of which the first is mediated by inosine monophosphate dehydrogenase (IMPDH) (Wigglesworth et al., 2013) **[Figure 10]**. The precise timing of meiotic resumption is then triggered by the preovulatory LH surge, which induces cumulus expansion, a process involving the synthesis of a hyaluronan-rich extracellular matrix. Cumulus expansion requires stimulation by FSH or EGF-like peptides and the activation of the MAPK3/1 and MAPK14 kinase signalling pathways in CCs. The consequent interruption of cGMP supply activates PDE3A, reduces intraoocyte cAMP, and GVB, the first morphological hallmark of meiotic resumption (Eppig, 1982).

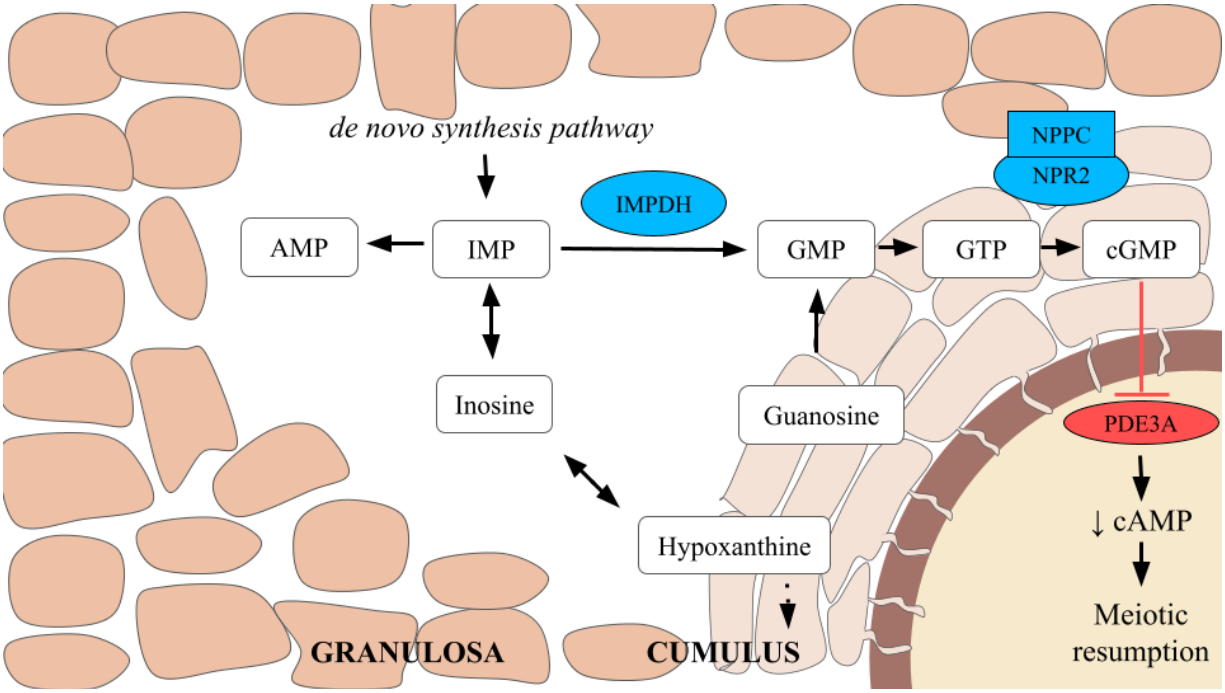

Figure 10 cGMP-mediated inhibition of PDE3A maintains meiotic arrest in the oocyte (adapted from Wigglesworth K, 2013)

The heterogeneity in developmental competence observed among oocytes retrieved from the same ovarian cohort can therefore be substantially attributed to variation in the functional state of their respective cumulus compartments. CCs exhibiting signs of metabolic dysfunction, altered responsiveness to GDF9/BMP15, premature gap junctional uncoupling, or dysregulated gene expression are consistently associated with oocytes of reduced quality and poorer embryological

outcomes (Ozturk, 2025). This tight association between the molecular state of CCs and oocyte developmental potential forms the conceptual foundation for their use as non-invasive reporters of oocyte quality in clinical settings (Uyar et al., 2013), and opens promising perspectives for exploiting their paracrine secretome, including soluble factors and EVs, to enhance in vitro maturation or rescue developmentally compromised oocytes in assisted reproductive technologies (Nikoloff, 2021; Sudewo et al., 2025).

1.3 Clinical applications of cumulus cells in assisted reproduction

The biological framework mentioned above, in which CCs emerge as active orchestrators of oocyte developmental competence rather than just structural accessories, carries profound implications for clinical practice. If the molecular state of CCs accurately reflects the quality of the oocyte they surround, then CCs themselves become a uniquely accessible tool, that can be interrogated without disturbing the gamete. This possibility has opened new research avenues aimed at harnessing the informative and functional potential of CCs in the context of assisted reproductive technologies (ART).

CC gene expression profiles were tested as non-invasive biomarkers for oocyte quality assessment, for the identification of candidate markers (transcripts or proteins) capable of predicting fertilization, embryo development, and pregnancy outcomes. Also, the role of CCs as a functional feeder layer in *in vitro* maturation (IVM) protocols has been investigated, illustrating how the presence and quality of CCs during IVM critically determines the developmental competence of the resulting oocytes. Finally, EV- and miRNA-mediated cumulus-oocyte communication has been deeply studied, exploring how miRNA profiling of follicular fluid EVs may serve both as a diagnostic tool and as a potential therapeutic strategy to enhance oocyte competence in ART settings. A brief description of these approaches is hereafter reported.

1.3.1 CCs as non-invasive biomarkers for prediction of oocyte quality

The main purpose of ART centres is the safe and rapid discrimination, from a pool, of high-quality oocytes and embryos which have the ability to generate good blastocyst and further healthy baby. This selection is normally based on morphological and morphokinetic features of the oocyte as ZP thickness, cytoplasmatic granularity, cleavage rate, fragmentation degree and polar body extrusion. Despite these have been the most used selection methods till these years, it has been seen that they

are not so accurate in predicting oocyte and embryo health; in fact, a big proportion of morphologically normal embryos had chromosomes abnormalities. This highlights the need to discover and develop new assays that are objective, accurate, fast, consistent and affordable , in order to increase implantation success and reduce the cost and the time needed. Furthermore, some invasive procedures may interfere with oocyte and embryo viability. In this context, the use of CCs as non-invasive biomarkers to assess developmental competence of oocytes and the resulting embryo is considered. They represent the primary target because they are typically discarded after the harvesting of denuded oocyte [**Figure 11**] and they are suitable for several molecular and biochemical analyses. Importantly, CCs share the same microenvironment as the oocyte and closely reflect its maturation status, making them a biologically relevant for evaluating oocyte health (Ozturk, 2025).

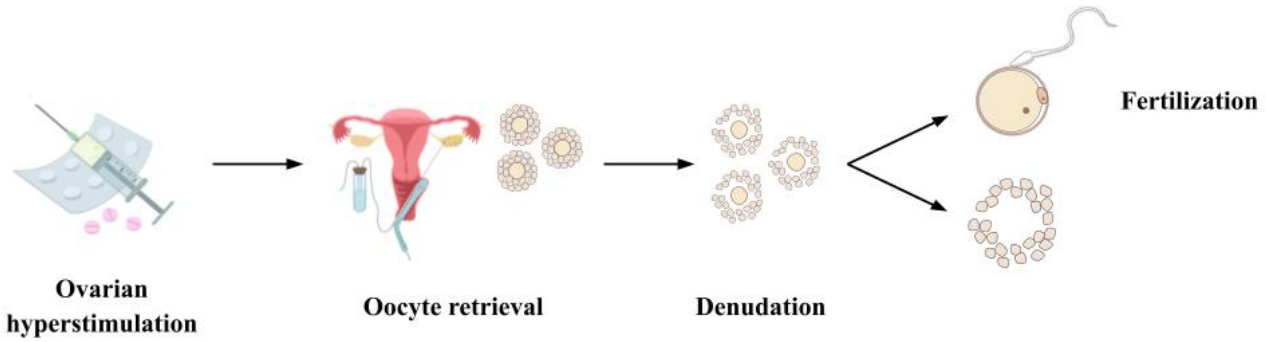

Figure 11 Main steps of assisted reproductive technology (ART): following ovarian hyperstimulation and oocyte retrieval, cumulus cells are removed during denudation and discarded, leaving the denuded oocyte available for fertilization

Transcriptomic approaches have emerged as one of the most promising strategies to exploit the informative potential of CCs. Novel embryo assessment strategies take advantage of rapidly developing transcriptomic technologies to explore the gene expression profile of CCs in association with clinically outcomes. Two main methodological approaches have been pursued: quantitative reverse transcription PCR (*q*RT-PCR) for the analysis of individual candidate genes, microarray or RNA sequencing technologies for genome-wide expression profiling. Studies using *q*RT-PCR have identified several CC-expressed genes associated with oocyte maturation, fertilization and embryo quality, as well as pregnancy outcomes. The most relevant reported candidates are PTGS2, HAS2, GREM1, VCAN, AREG, STAR, and CAMK1D. Also, a systematic analysis of these genetic biomarkers has confirmed their association with distinct clinical outcomes: CAMK1D, PFKP, HAS2, VCAN, GDF9, BMP15, and PTGS2 correlate with oocyte quality; GREM1, PTGS2, and HAS2 with embryo quality; and GDF9, BMP15, and VCAN with pregnancy rate (Massoud et al., 2024). Notably, a study reported that PTGS2, HAS2, and GREM1 were significantly upregulated in CCs surrounding

oocytes that developed into high-grade day 3 embryos. More recently, multi-gene predictive models combining CC transcript levels with clinical parameters has been developed, achieving pregnancy prediction with a sensitivity of 70% and a specificity of 90%. However, the reproducibility of individual gene markers across studies remains limited, largely due to inter-patient variability and differences in ovarian stimulation protocols, highlighting the need for standardized and validated panels rather than single-gene approaches. Genome-wide microarray analyses have allowed a more unbiased and comprehensive characterization of the CC transcriptome. Several studies have identified hundreds of differentially expressed genes between CCs associated with competent versus incompetent oocytes, involved in processes such as cell cycle regulation, angiogenesis, apoptosis, metabolic activity, and response to hypoxic conditions. Among the validated candidates, RGS2 has been associated with oocyte developmental competence and clinical pregnancy, while SPSB2 has been proposed as a potential indirect marker of oocyte aneuploidy, raising the prospect of using CC transcriptomics as a non-invasive alternative to invasive preimplantation genetic testing (Assou et al., 2010; Uyar et al., 2013).

In addition, new parameters have been discovered as potential biomarkers of oocyte and embryo quality still using CCs. One example is the evaluation of telomere length. Variability in the relative telomere length of individual CCs has been reported, correlating with oocyte maturation, fertilization rates in young infertile women, and embryo quality in patients undergoing IVF. Notably, shorter telomeres were observed in CCs associated with immature oocytes, unfertilized eggs, and poor-quality embryos. All together, these data suggest that the relative telomere length in individual CCs may serve as a promising biomarker for the selection of embryos designated for implantation (Cheng et al., 2013).

1.3.2 Co-colture: CC as feeder layer for oocyte in vitro maturation

In vitro maturation (IVM) represents a promising alternative to conventional ovarian stimulation protocols in ART, especially in the context of fertility preservation and in patients at risk of ovarian hyperstimulation syndrome (OHSS). However, the developmental competence of *in vitro*-matured oocytes remains suboptimal compared to their in vivo counterparts, highlighting the need for improved culture systems that better recapitulate the follicular microenvironment (Jurema & Nogueira, 2006). In this respect, several studies demonstrate that CCs are fundamental for replicating the real follicular microenvironment, and that the proportion of mature and developmentally competent oocytes cultured in the absence of CCs is lower compared to those cultured with them. This type of maturation can be performed directly with non-denuded antral follicles, denuded only

just before ICSI (Sanchez et al., 2019), or alternatively, GV oocytes can be denuded and placed onto a feeder layer of CCs (Cavalera et al., 2019).

This last study demonstrated that IVM of mouse GV oocytes upon a feeder layer of selected CCs significantly enhances their developmental competence, highlighting the importance of not only the presence of CCs, but also their selection, suggesting that the quality and functional state of the feeder layer are critical determinants of IVM outcomes. Notably, feeder layers prepared from developmentally competent CCs supported blastocyst development rates comparable to those obtained with intact COCs, whereas oocytes matured on incompetent feeder displayed severely impaired developmental potential [**Figure 12**]. These findings establish a reliable culture platform for the further optimisation of IVM protocols for denuded oocytes, and provide a valuable experimental model to elucidate the molecular mechanisms underlying the bidirectional cross-talk between the oocyte and its surrounding CCs during the GV to metaphase II (MII) transition. Furthermore, these results suggest that CCs retain their ability to support oocyte maturation *in vitro* even after losing their direct physical connection with the oocyte, possibly through the release of paracrine factors that could be further exploited to improve ART outcomes (Cavalera et al., 2019).

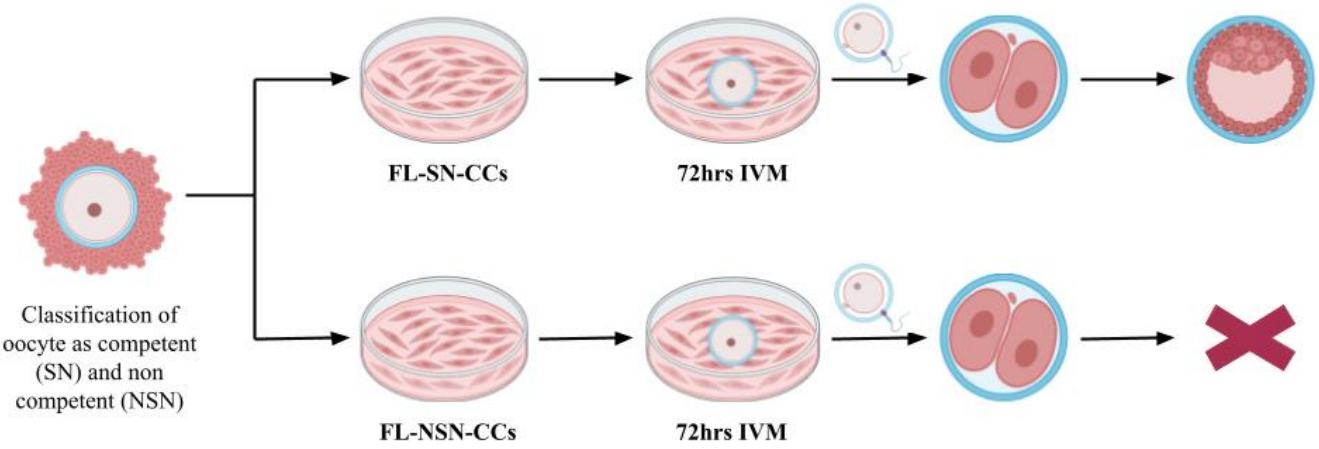

Figure 12 Schematic representation of the IVM experimental design in which denuded GV-stage mouse oocytes are matured on feeder layers of either competent (FL-SN-CCs) or non-competent (FL-NSN-CCs) CCs and the outcomes (adapted from Cavalera et al., 2019)

1.3.3 EVs and miRNAs in cumulus-oocyte communication: potential applications in ART

Within the follicle, several molecules, ribonucleoproteins, proteins and organelles are continuously exchanged between the oocyte and the surrounding CCs. This bidirectional communication can occur either through direct cell-to-cell contact or via EVs, which are broadly classified into macrovesicles

(MVs) and exosomes (EXOs). Upon fusion of multivesicular body with the plasma membrane, these vesicles are released into the extracellular space (da Silveira et al., 2018).

Accumulating evidence suggests that miRNAs play a key regulatory role in pathways governing follicular growth, dominance, atresia and, critically, the acquisition of oocyte developmental competence (da Silveira et al., 2018; Fiorentino et al., 2024).

To further investigate the molecular determinants of oocyte competence, comparative miRNA profiling of EVs secreted under competent and non-competent CC conditions revealed distinct miRNA signatures, with a subset of differentially expressed miRNAs likely actively modulating the expression of genes contributing to oocyte developmental competence (Fiorentino et al., 2024).

From a translational perspective, these results open promising possibilities for clinical applications in ART along two complementary directions. First, miRNA profiling of follicular fluid EVs has been proposed as a non-invasive strategy to assess oocyte quality without compromising the cumulus-oocyte complex and the miRNA candidates identified here could serve as molecular biomarkers to predict oocyte developmental potential, potentially improving embryo selection and overall IVF outcomes (Santonocito et al., 2014; Scalici et al., 2016). Second, and perhaps more ambitiously, the supplementation of specific miRNAs during IVM could represent a novel strategy to rescue developmentally compromised oocytes, restoring or enhancing their competence and improving blastocyst yields (Esposito et al., 2026). Similar approaches have already been explored in somatic cell contexts, where exogenous miRNA delivery has been shown to modulate gene expression and cellular function effectively (Kim et al., 2013). If validated in the oocyte system, this strategy could offer a targeted, minimally invasive tool to improve the quality of oocytes that would otherwise be discarded in clinical ART settings. However, the functional role of the identified miRNAs remains to be experimentally verified (Fiorentino et al., 2024).

2. Aim of the study

As the role of CCs during the folliculogenesis and the maturation of the female gamete has been clearly evidenced, as well as their potential applications *in vitro* to predict or sustain oocyte developmental competence, the overarching goal of this master's thesis was to deepen our understanding of cumulus cell biology by pursuing a two-fold strategy: 1) identifying predictive molecular biomarkers of embryonic success; and 2) optimizing a standardized long-term *in vitro* cumulus cells culture.

To achieve this purpose, the project was structured into two specific aims:

Aim 1: miRNome profiling of human cumulus cell-derived extracellular vesicles. The first aim is the characterization of the miRNA cargo within EVs secreted by human CCs isolated from individual COCs. A comparative analysis was performed between EVs produced by CCs associated with oocytes that successfully progressed to the blastocyst stage after fertilization, and those that failed to reach blastocyst development. The ultimate goal was to identify specific differentially expressed miRNAs that could serve as non-invasive biomarkers of oocyte competence and embryonic quality.

Aim 2: Establishment and characterization of a long-term culture of murine cumulus cells. The second aim sought to break past the traditional 3-day culture barrier by establishing a long-term primary cell culture utilizing mouse CCs. To evaluate the preservation of cell quality and lineage identity over extended passages, the culture was comprehensively characterized using morphological and morphometric parameters, cellular senescence and the expression of lineage-specific markers.

3. Materials and Methods

3.1 Part 1 - *miRNome profiling of human cumulus cell-derived extracellular vesicles*

3.1.1 Isolation of human CCs

Human CCs were isolated at the Genera PMA Assisted Reproduction Clinic in Rome from COCs of 61 women (mean age 38.7±3.1 years; BMI 20.9±5.1 kg/m2) who signed the informed consent form, without ovarian pathologies, undergoing IVF (December 2023-July 2025) after ovarian stimulation and with normozoospermic partners. COCs pick-up was made through aspiration from the ovary and the oocyte denudation from CCs was performed in single 50 µl drop of albumin-HEPES medium containing 20 IU/mL hyaluronidase (Hyale). CCs from single COCs were cryopreserved separately in a medium containing 10% DMSO in Bovine Fetal Serum (FBS; Gibco). CCs from each tube were classified based on the ability of their corresponding oocyte to reach blastocyst stage following fertilization. Specifically, CCs derived from oocytes that successfully developed to blastocyst stage after fertilization were classified as BLASTO (BL), whereas those from oocytes that failed to reach the blastocyst stage were named as No-BLASTO (NoBL). The single tubes, sent to the Laboratory of Biology and Biotechnology of Reproduction of the University of Pavia, were maintained in liquid nitrogen until their use.

3.1.2 In vitro culture of human CCs

To ensure an adequate cell concentration for subsequent culturing and to reduce individual biological variability, CCs from three independent tubes, each originating from a different patient, were pooled together. Through this approach, both BLASTO-cumulus cell (BL-CC) and No-BLASTO-cumulus cell (NoBL-CC) cultures were successfully established following this protocol.

Three frozen cell aliquots were defrosted in a 37 °C water bath, in less than 3 minutes to avoid damages. Cells were collected into a tube containing 3 mL of pre-warmed maturation medium (MM; α-MEM-Glutamax enriched with 15% FBS (Gibco), 25.3 µg/mL sodium pyruvate (Sigma-Aldrich), 100 IU/mL penicillin /75 µg/mL streptomycin, and 1 mg/mL fetuin (Sigma-Aldrich). Samples were centrifuged at 500 rcf for 5 minutes, the supernatant was eliminated and the pellet resuspended in 300 µL of MM. The cells, seeded in 96-well plates at 37°C, 5% CO_2 with 200 µl of MM changed every day, were cultured for 3 days.

3.1.3 EVs retrieval and isolation

CCs were washed three times with 200 µL of pre-equilibrated exosome-free medium [EXO-free M; α-MEM-Glutamax containing 5% exosome-depleted FBS (Gibco), 25.3 µg/mL sodium pyruvate (Sigma-Aldrich), 100 IU/mL penicillin / 75 µg/mL streptomycin, 50 mU/mL FSH (Sigma-Aldrich) and 5 ng/mL EGF (Sigma-Aldrich)] and cultured for 24 hrs at 37 °C and 5% CO_2 in 50 µL of EXO-free M. After, the medium was recovered from each well and either it was cryoconserved at -80°C or transferred into ultra-clear centrifuge tubes and centrifuged at 100 000 x g for 60 minutes at 4°C using an Ultra-High-Speed Centrifuge Optima MAX-XP (Beckman Coulter). The obtained pellet was resuspended in 50 mL of sterile PBS or exosome-depleted α-MEM–Glutamax medium for further analyses.

3.1.4 Microarray transcriptome profiling analysis

The samples were analysed in collaboration with Professor Valentina Gatta of the University of Chieti-Pescara. MiRNAs were extracted using the Total Exosome RNA and Protein Isolation Kit following the manufacture's instructions and subsequently processed for microarray transcriptome profiling analysis on a GeneChip System 3000 platform.

To identify differentially expressed miRNAs between the BL group vsNoBL group, bioinformatic analysis was performed on the microarray dataset. The filtering criteria for statistical and biological significance were set at a Gene-Level Fold Change (FC) of < -2 or > 2 and a Gene-Level P-Value of < 0.05, calculated using the empirical Bayes ANOVA method (*ebayes*). Signal detectability was restricted by considering a probeset actively expressed only if > 50% of the samples exhibited a *Detection Above Background* (DABG) value below 0.05.

3.1.5 Literature-based screening and selection of ovarian-related miRNAs

To prioritize the most biologically relevant candidates from the total pool of differentially expressed miRNAs obtained by microarray analysis, an extensive literature-based screening was performed. The literature search was conducted on each differentially expressed miRNA, searching on Pubmed its correlation with the following specific keywords: *ovary* or *ovarian*, *folliculogenesis*, *ovarian follicle*, *cumulus cells*, *granulosa cells*, *oogenesis*, *meiosis*, *pre-implantation*, *IVF*, *embryo*, *oocyte*, *fertilization* and *blastocyst*. Only miRNAs with documented functional roles in these reproductive processes were selected for subsequent downstream target gene identification.

3.1.6 Diana tools identification of human EVs-miRNA target genes

To identify the miRNA target genes the "mirPath v.4" database on the DIANA tools website (http://www.microrna.gr/miRPathv4; Tastsoglou et al., 2023) was exploited. The investigation was limited to *Homo Sapiens* and made using the 4 databases: TarBase v.8 and miRTarBase 2022 documented interactions that have been experimentally validated, while DIANA-microT-CDS 2023 and TargetScan 8 employed prediction algorithms to identify target genes. Genes associated with relevant pathways related to the processes of folliculogenesis and oocyte maturation were further investigated through a bibliographic search on PubMed. Each gene of interest was cross-referenced with the following keywords: *ovary*, *folliculogenesis*, *ovarian follicle*, *CCs*, *oocyte*, *oogenesis*, *meiosis*, *fertilization*, *developmental competence* and *preimplantation*. References were restricted to the Mammals class.

3.1.7 KEGG identification of pathways related to human EVs-miRNA target genes

To connect the identified genes to their associated pathways, a bioinformatics analysis was conducted through R studio using the KEGG (Kyoto Encyclopedia of Genes and Genomes) database.

3.2 Part 2 - *Establishment and characterization of a long-term culture of murine cumulus cells*

3.2.1 Isolation and culture of mouse CCs

COCs were obtained from 4-week-old CD1 female mice, purchased from Charles River (Lecco, Italy). Female mice were injected 48 hrs earlier the sacrifice with ten IU Folligon (Intervet Productions Srl). Only mature antral COCs were collected from isolated ovaries. CCs and oocyte were manually separated through mouth pipetting. Mouse CCs were obtained from 15 unclassified COCs and seeded in 96-well plates. They were maintained at 37°C, 5% CO_2 in 200 µl of MM, changed every two days. CCs were maintained in culture for 24 days. At day 1, 2, 3, 8, and 24, live-cell images were acquired using an inverted Olympus IX71 microscope equipped with an INFINITY2-1C camera. For CCs subjected to immunofluorescence analyses, cells were directly seeded and cultured on 12 mm in diameter glass slides under the same conditions described above. At day 3, 8, 13, 18, and 24 of culture, cells were either fixed for immunofluorescence analysis or lysed for RNA extraction.

3.2.2 Immunofluorescence

CCs were fixed directly on glass slides after 3, 8, 13, 18 and 24 days of culture in 500 µL of 4% paraformaldehyde in 1X PBS and stored at 4°C until use. The cells were washed twice with 500 µL of 1X PBS for 5 minutes under gentle agitation, followed by permeabilization with 500 µL of 0.2% Triton in 1X PBS for 10 minutes. Then cells were blocked with 500 µL of blocking buffer (1% BSA, 0.01% Tween in PBS) for 20 minutes.

For Lamin B1 staining, cells were incubated overnight at 4°C with an Anti-Lamin B1 rabbit polyclonal IgG antibody (Santa Cruz Biotechnology), used at 1:150 dilution in 1X PBS. After three washes with 500 µL of 1X PBS for 5 minutes under gentle agitation, cells were incubated with an Alexa Fluor 555-conjugated anti-rabbit secondary antibody (Invitrogen), diluted 1:300 in 1X PBS for 90 minutes at 37°C.

For F-actin staining, cells were incubated with tetramethylrhodamine B isothiocyanate (TRITC)-conjugated phalloidin (Sigma-Aldrich) diluted 1:250 in 1X PBS for 90 minutes at 37°C.

Following the incubation steps, all samples were washed three times with 500 µL of 1X PBS for 5 minutes under gentle agitation and incubated with 0.2 µg/mL DAPI for 10 minutes. After two additional washes with 500 µL of 1X PBS for 5 minutes under gentle agitation, glass slides were mounted upside down with a drop of DABCO and stored in the dark until image acquisition.

3.2.3 Images acquisition and elaboration

Lamin B1-marked cell's images were obtained using a 40X objective of a confocal Leica SP8 light microscope equipped with a motorized XY scanning stage controlled by the LAS X Navigator stitching Lite version software (Leica).

Phalloidin-marked cells' images were obtained using a 60X objective of a fluorescent microscope Olympus BX6C equipped with motorized z-stack (MFD Olympus B41/51 with Tango1-Descktop controller) connected to a camera (CCD Olympus DP72) controlled by CellSense™ software.

The images were subsequently analysed with the Fiji and MATLAB® programmes.

3.2.4 Analysis of CCs morphometric and morphological parameters

The "*gastruloid_morphology*" algorithm (Rebuzzini et al., 2024) was used to quantify the area and perimeter (morphometric features), circularity, eccentricity and elongation (morphological features) of CCs following Phalloidin labelling.

The morphological features of each single cell were defined by the following parameters: a) Circularity, comprised between 0 and 1, where the value 0 represents an ellipse, whereas the value 1 represents a circumference; b) Elongation is a form factor; an elongation equal to 1 represents a circumference, whereas an elongation >1 represents an ellipse; c) Eccentricity, ranged from 0 to 1, specifies the eccentricity of the ellipse with the same second-moments as the cellular region. It is calculated as the ratio of the distance between the foci and the major axis length, where a value of 0 represents a perfect circle (Sutcliffe et al., 2018).

3.2.5 RNA extraction from CCs during culture

RNA was extracted from CCs, at day 3, 8, 13, 18 and 24 of culture using the miRNeasy Micro Kit (Qiagen), following manufacturer's instructions. Briefly, the lysis of the cells was performed directly in the well and, following the addition of chloroform, the homogenate was separated into aqueous and organic phases by centrifugation at 13 000 x g for 15 minutes at 4°C. The RNA-containing aqueous phase (upper phase) was extracted using absolute ethanol and the sample was transferred to the RNeasy MinElute spin column, where RNA bound the membrane while other contaminants were washed away. RNA was eluted in 14 μL of RNase-free water. The RNA samples were stored at -20°C.

3.2.6 Reverse transcription

The reverse transcription reaction was carried out in a final volume of 20 µl, containing 5 µl of RNA sample, 8 mM dNTPs (Invitrogen), 50 U of MuLV reverse transcriptase (Invitrogen), 20 U of RNasin RNase inhibitor (Promega), 0.625 µM oligo(dT) primer (Roche), 1.875 µM random hexamers (RH; Invitrogen), 1x First Strand Buffer (Invitrogen), and 5 mM DTT (Invitrogen). The reaction was run in a thermocycler under the following cycling conditions: an initial annealing step at 25°C for 10 minutes, followed by reverse transcription at 50°C for 50 minutes, and a final inactivation step at 70°C for 15 minutes to inactivate the MuLV reverse transcriptase, for a total reaction time of 75 minutes. The cDNA was stored at -4°C.

3.2.7 qRT-PCR

The *q*RT-PCR was performed in a total volume of 20 µl, containing 5 µl of cDNA (appropriatelydiluted with H_2O), 1x SYBR Green Master Mix (Invitrogen), 200 nM of each primer (Eurogentec). The expression of *Has2* and *Ptx3* was assessed, using *β2-microglobulin* (B2M) as the housekeeping gene for normalization. The primer sequence is reported in ***Table 1***.

Table 1 Primer sequences and amplicon length (bp)

Primers	Sequence	Amplicon length (bp)
Has2 F	5'-AAGACCCTATGGTTGGAGGTG-3'	95
Has2 R	5'-CATCCAGTATCTCACGCTGCT-3'	
Ptx3 F	5'-TGGACAACGAAATAGACAATGG-3'	95
Ptx3 R	5'-GATGAACAGCTTGTCCCACTC-3'	
B2M F	5' GAATTCACCCCCACTGAGACT 3'	103
B2M R	5' TGCTTGATCACATGTCTCGAT 3'	

The thermocycler protocol consisted of an initial denaturation step at 95°C for 5 minutes, followed by 40 cycles at 95°C for 10 seconds, 60°C for 15 seconds, and at 72°C for 20 seconds. A melting curve analysis was performed at the end of the run, with a temperature gradient from 50°C to 95°C, to verify the specificity of the amplification products.

3.2.8 Statistical analysis

The statistical analyses were performed using R studio. For the quantitative analysis of Lamin B1 expression categories across time points, a Chi-square test of independence was applied, while the Kruskal-Wallis test with Dunn's post hoc test was used for the evaluation of non-parametric morphometric and morphological parameters. Instead, gene expression levels were evaluated via one-way ANOVA.

4. Results

4.1 Part 1 - *miRNome profiling of human cumulus cell-derived extracellular vesicles*

4.1.1 Analysis of human EVs miRNA content

Microarray analysis was performed to identify the miRNA cargo of EVs secreted by BL-CCs and NoBL-CCs cultures. The expression profile was evaluated across a total of 4,506 miRNA sequences. Among these, 90 miRNAs were significantly differentially expressed when comparing BL vs NoBL, with 86 being down-regulated and 4 up-regulated [**Figure 13**].

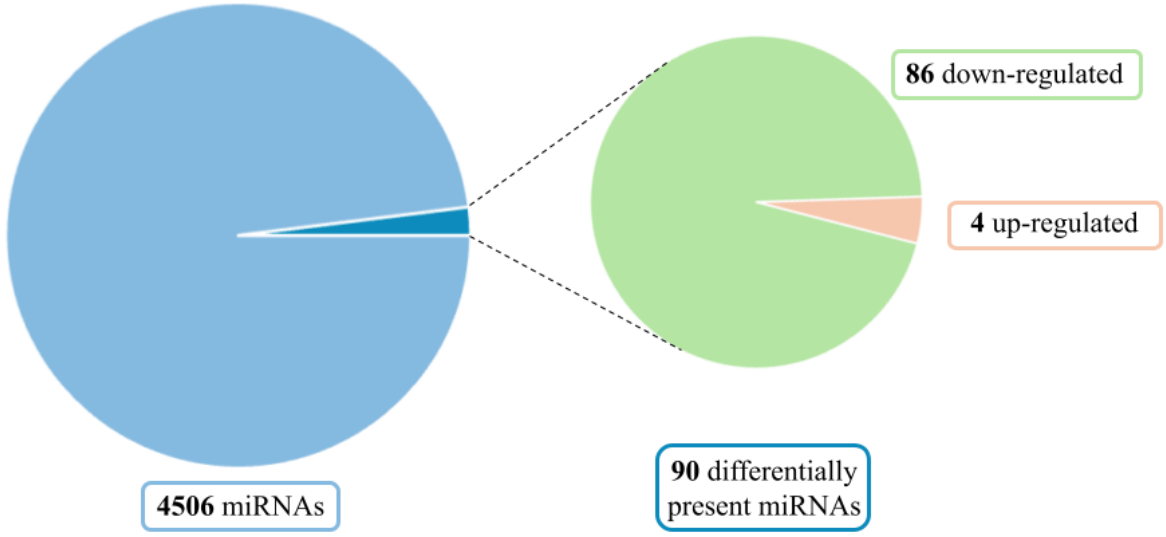

Figure 13 Differential miRNA expression in human cumulus cell-derived EVs

Furthermore, a literature search was conducted via PubMed to cross-reference the 90 differentially expressed miRNAs with the following key words: *ovary* or *ovarian*, *folliculogenesis*, *ovarian follicle*, *cumulus cells*, *granulosa cells*, *oogenesis*, *oocyte*, *meiosis*, *fertilization*, *pre-implantation*, *IVF*, *embryo* or *blastocyst*. This analysis revealed that 24 of these miRNAs [**Table 2**], all down regulated, were already known to be associated with ovarian functions including meiosis resumption, fertilization, follicle growth, and acquisition of oocyte developmental competence. Specifically, 41% of them had been studied in humans, 18% in rodents, 17% in bovines, 10% in porcines, 9% in ovines, and 4% in equines [**Figure 14**].

Table 2 Comprehensive annotation of the 24 relevant human miRNAs and their target genes

miRNA Name	Target Genes
hsa-let-7b-5p	401
hsa-let-7i-5p	348
hsa-miR-24-3p	258
hsa-miR-93-5p	432
hsa-miR-132-3p	205
hsa-miR-193b-5p	720
hsa-miR-202-3p	375
hsa-miR-204-3p	754
hsa-miR-206	120
hsa-miR-320d	267
hsa-miR-338-5p	665
hsa-miR-382-5p	22
hsa-miR-423-3p	33
hsa-miR-503-5p	116
hsa-miR-509-3p	332
hsa-miR-574-5p	480
hsa-miR-885-3p	395
hsa-miR-1207-5p	631
hsa-miR-1246	572
hsa-miR-1261	206
hsa-miR-1290	361
hsa-miR-4463	256
hsa-miR-4523	21
hsa-miR-4651	1054

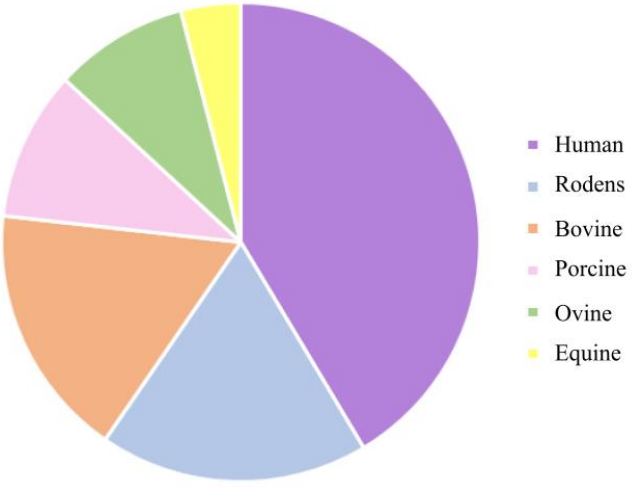

Figure 14 Distribution across species of the 24 identified miRNAs known to be involved in ovarian processes

4.1.2 Identification of miRNA target genes and pathway

Based on the 24 selected miRNAs, a downstream bioinformatic analysis and bibliographic searches were conducted. Utilizing the DIANA-miRPath v4.0 database, a total of 1,612 target genes were identified through either experimentally validated interactions or prediction algorithms and associated with different miRNAs [**Table 2**].

Bibliographic analysis was further carried out identifying a subset of 293 genes. These genes were found to be functionally associated with key processes including: pre-implantation embryo development (N = 104 genes), oocyte maturation (N = 60 genes), meiotic resumption (N = 60 genes), acquisition of developmental competence (N = 34 genes), cumulus expansion (N = 30 genes), ovulation (N = 30) and fertilization (N = 20) [**Figure 15**]. Since various genes mapped to multiple functional categories, this outcome pointed out the highly intricate regulation underlying developmental processes.

KEGG pathway enrichment analysis identified several pathways known to be pivotal for oocyte growth and maturation. In particular, significant enrichment was found for the TGF-β (N = 34 genes), PI3K–Akt (N = 55 genes), MAPK (N = 59 genes), Hippo (N = 36 genes), Ras (N = 43 genes), Rap1 (N = 42 genes), and cAMP (N = 42 genes) signalling transduction pathways. Additionally, the analysis highlighted key molecular cascades directly related to oocyte meiosis (N = 39), progesterone-mediated oocyte maturation (N = 34), regulation of the actin cytoskeleton (N = 43), and cell cycle control (N = 53) [**Figure 16**].

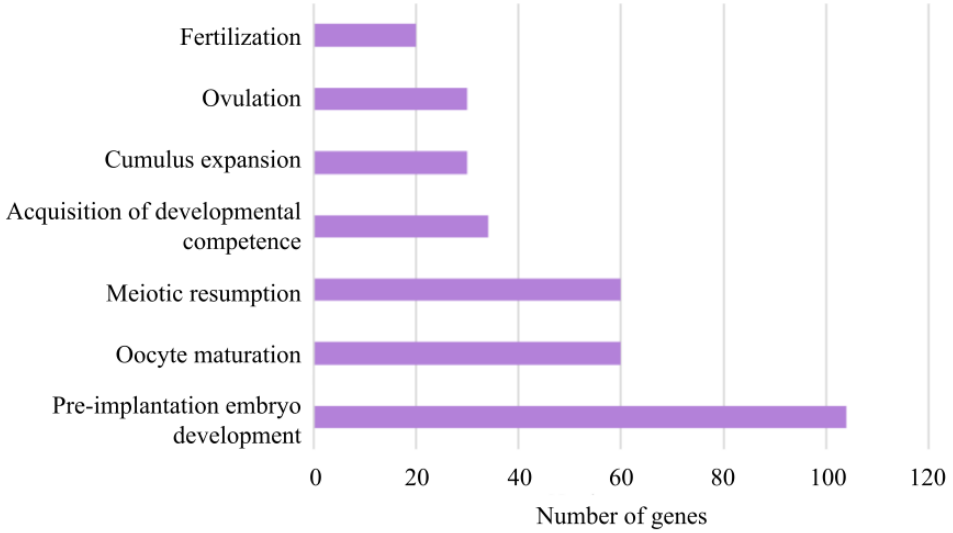

Figure 15 Distribution of the 293 subset genes across major ovarian and embryological functions identified via literature search

Figure 16 Functional annotation of the 293 target genes via KEGG database

4.1.3 Functional convergence between human and mouse

A comparison between the 293 gene targets of the 24 human miRNAs identified in this study and the 71 of the 7 mouse miRNAs from the work of Fiorentino et al. (2024) revealed 55 target genes in common between the two species [**Figure 17**]. These common genes are actively involved in cumulus expansion, fertilization, meiotic resumption, and developmental competence [**Figure 18**].

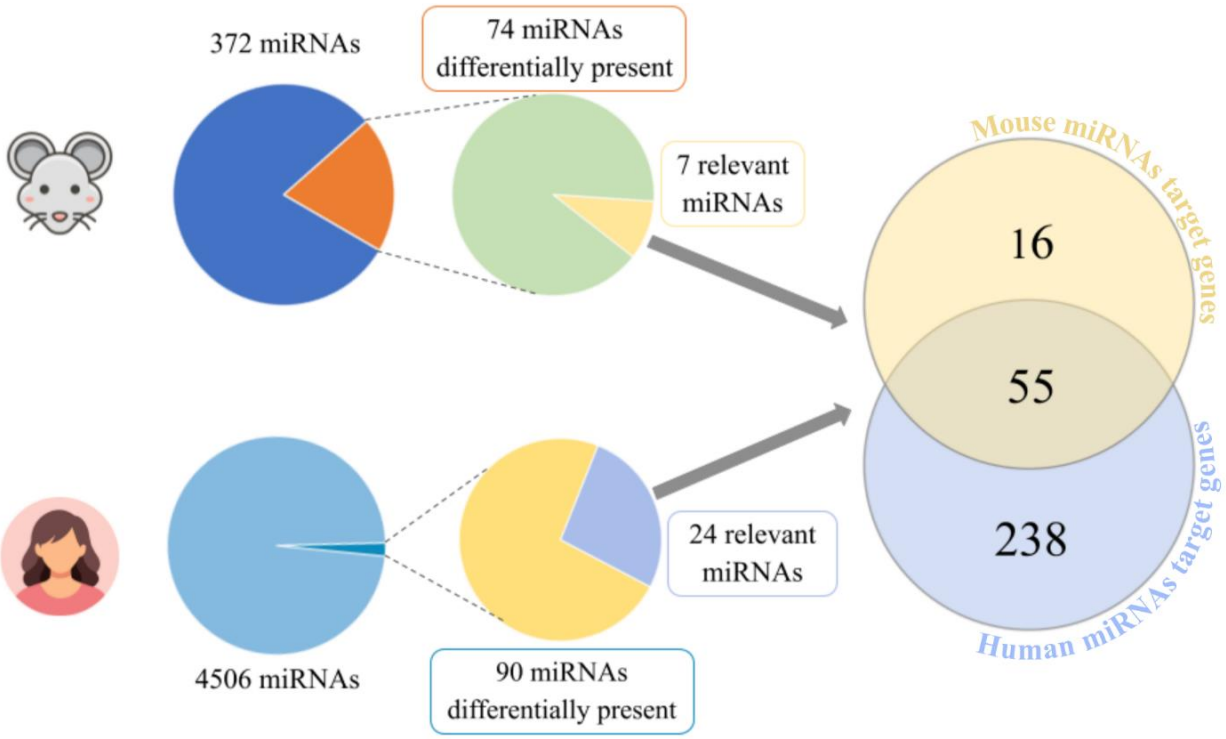

Figure 17 Graphical representation of the miRNA selection pipeline for mouse and human datasets. The Venn diagram illustrates that among the target genes, a subset of 55 genes is shared between the two analysed species

55 convergence genes
AR, BMP4, BMPR2, CCND2, COL1A1, CREB1, CTGF, CXCL12, E2F1, ERBB4, FOXO1, GJA1, MDM2, MMP2, SMAD4, TGFBR1, YAP1, PLCB1, ACTB, APC, ARF6, CDC14B, CDC42, CDK4, FZR1, HDAC2, HIF1A, LIMK1, PAK1, PAK2, PAK4, PDE3A, PTK2B, RAB14, RAB8A, RALB, RHOA, SIRT1, ADIPOR2, AKT1, CAMK1D, CCNE1, CDK2, CUL1, ESR1, IRF1, KLF4, KRAS, LATS1, MYC, PARD6B, PFKP, PIKFYVE,SOS1, STAT3

CUMULUS EXPANSION

FERTILIZATION

MEIOTIC RESUMPTION

PREIMPLANTATION DEVELOPMENTAL COMPETENCE

Figure 18 Comprehensive list of the 55 conserved target genes shared between human and mouse datasets and their functional involvement

4.2 Part 2 - *Establishment and characterization of a long-term culture of murine cumulus cells*

4.2.1 Cumulus cells morphology observation during prolonged culture

The regular observation of the CC cell cultures over time revealed that CCs modified their morphology during culture. At earlier time points, specifically after 1 [**Figure 19A**] and 2 [**Figure 19B**] days of culture, the majority of cells attached to the plate and started to proliferate, acquiring a flattened and expanded morphology (arrowheads). A small fraction of cells retained a rounded morphology and appeared non-adherent to the culture plate, suggesting compromised viability. CCs required about 3 days of culture to reach 90% confluency [**Figure 19C**]. After 8 days of culture [**Figure 19D**], although the majority of cells seemed to maintain the morphology observed after 3 days of culture, characterized by a regular flatten shape, few cells start to undergo morphological changes, becoming larger and with dark granulation into the cytoplasm (arrow), suggesting the onset of phenotypic alterations associated with prolonged culture.

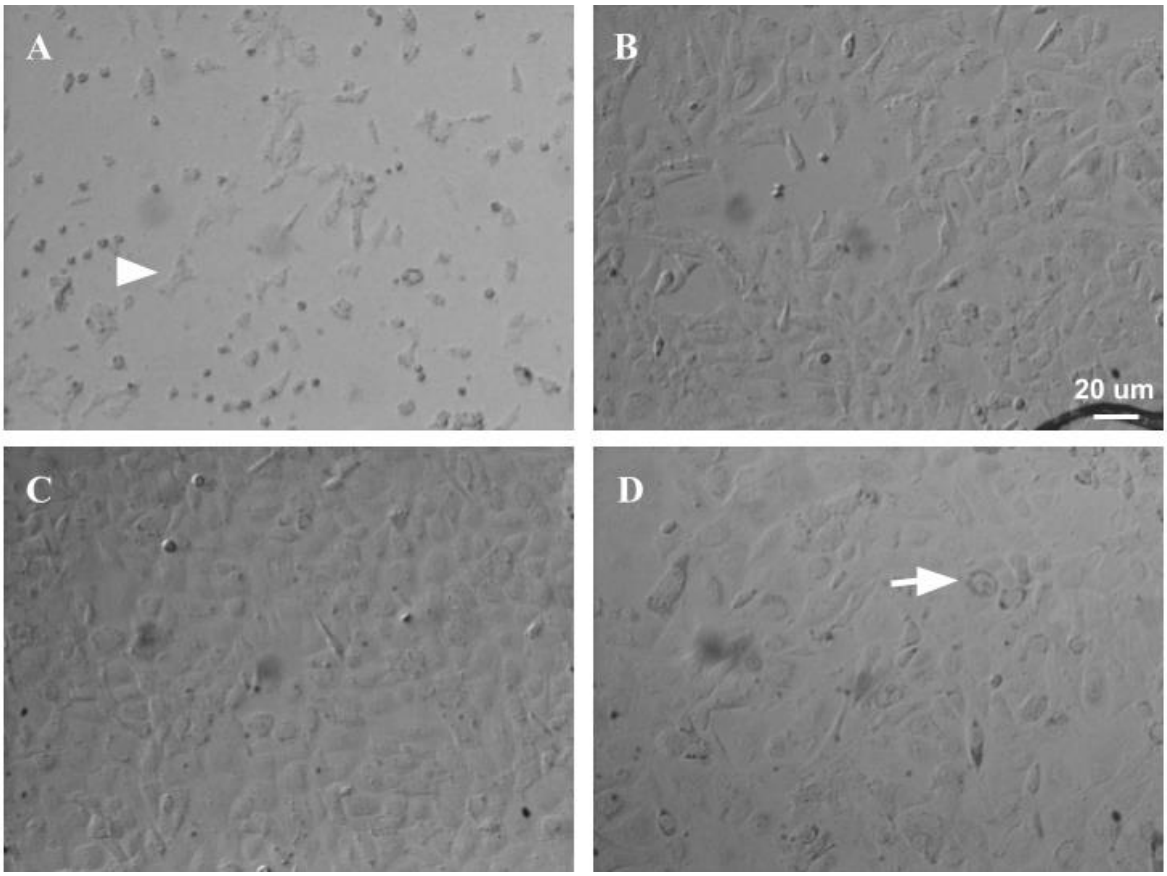

Figure 19 Representative images of CCs acquired at different time points during culture. A) 1, B) 2, C) 3 and D) 8 days of culture (10X magnification). Arrowhead indicates a cell displaying normal morphology, properly attached to the substrate; arrow indicates a cell undergoing morphological changes.

After 24 days of culture [**Figure 20**], massive morphological changes were observed across the cell population. Notably, a significant increase in cells displaying dense, dark cytoplasmic granulation was detected. These granulated cells progressively lost substrate adherence, shifting toward a small rounded morphology and appearing as dark spots detached or semi-detached from the plate (arrowheads). While a small fraction of cells retained a normal morphology, a subpopulation acquired a markedly elongated and enlarged senescent-like shape (arrows), thus losing the classic features typical of the cell population.

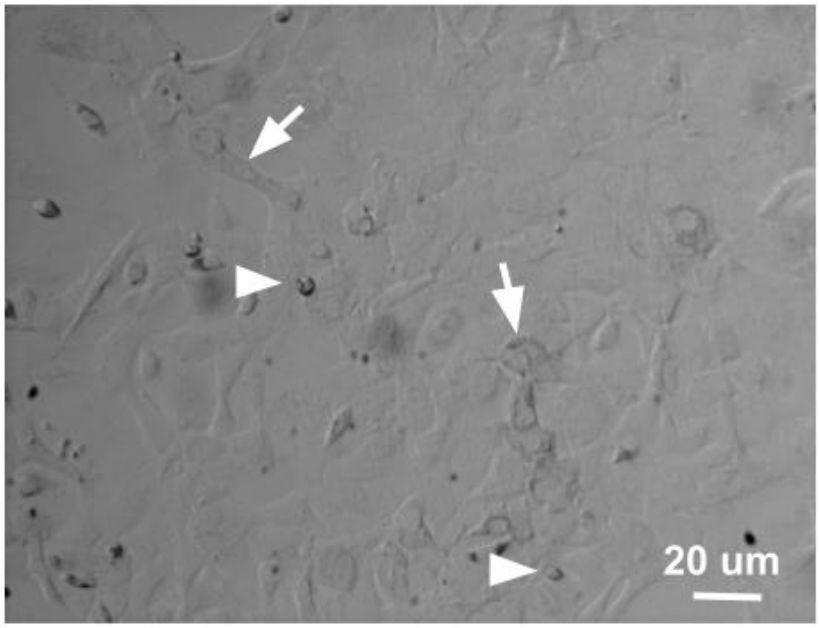

Figure 20 Representative images of CCs at day 24 of culture (10X magnification). Arrowheads indicate cells that are detached or undergoing detachment; arrows indicate cells undergoing morphological changes

4.2.2 Expression analysis of LAMIN B1

LAMIN B1 is a structural protein of the nuclear lamina that maintains nuclear shape and organizes chromatin within nucleus of eukaryotic cells (Gruenbaum et al., 2015). LAMIN B1 protein expression was analysed in CCs maintained in culture for 24 days, as it represents a robust marker of cellular senescence. Its downregulation represents a typical hallmark of the induction of cell senescence (Freund et al., 2015).

Analysis of confocal immunofluorescence images of CCs stained with an anti-LAMIN B1 antibody revealed progressive changes in signal distribution during long-term culture [**Figure 21**].

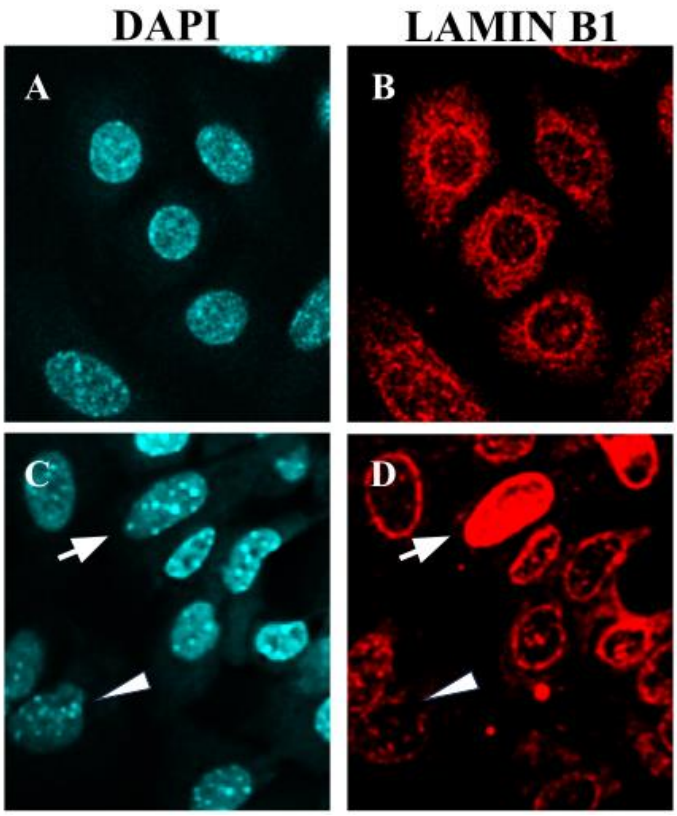

Figure 21 Representative immunofluorescence images of LAMIN B1 expression in CCs at 3 (A and B) and 24 (C and D) days of culture. Arrowhead indicates a cell which lacks of Lamin B1 signal; arrow indicates an example of cell with overexpression of Lamin B1

The collected images were analysed and the different subpoputations observed were counted. The results were reported in **Figure 22**.

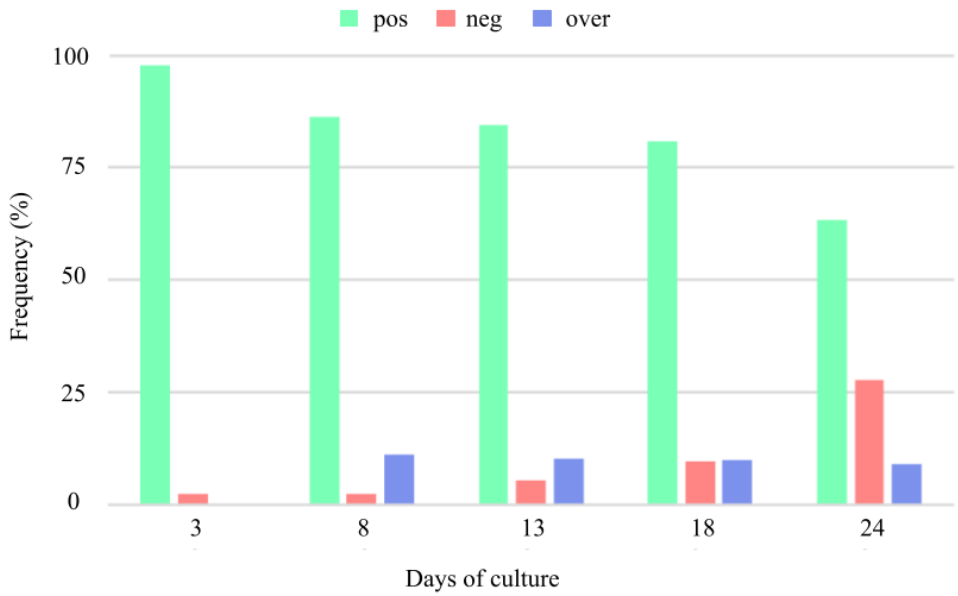

Figure 22 Frequency (%) of the cell populations exhibiting positive (pos), negative (neg), or overexpression (over) of Lamin B1 signals during CCs culture

Following 3 days of culture, the cell population appeared highly homogeneous, with almost all cells (>95%) displaying a uniform LAMIN B1 fluorescence signal characterized by a well-defined perinuclear ring [**Figure 21B and Figure 22**]. A small subpopulation characterized by the absence of the LAMIN B1 was detected, but with a very low percentage (about 2%). As culture time progressed, significant heterogeneity ($p < 0.001$) emerged within the cell population, leading to the progressive decline of the standard positive fraction and the concomitant appearance of two distinct alternative subpopulations [**Figure 21D** and **Figure 22**]. Specifically, the subpopulation characterized by a complete absence of the Lamin B1 signal became significantly detectable at day 13 (5,2%; $p < 0.001$=). This fraction showed an increase at day 18 (10%) and at day 24, sharply increasing to represent nearly 30% of the entire cell population [white arrowhead in **Figure 21C and Figure 21D;** red bars **Figure 22**]. In parallel, an overexpressing subpopulation emerged early in the timeline, showing a sharp initial increase at day 8, where it accounted for approximately 11% of the total population. In contrast to the negative fraction, this overexpressing subpopulation stabilized as a constant minority, fluctuating between 8% and 10% throughout the remaining culture period up to day 24 [white arrow in **Figure 21C and Figure 21D; Figure 22**]. As a consequence of the expansion of these two subpopulations, the percentage of standard positive cells [green bars in **Figure 22**] showed a progressive and steady decline over time, dropping from the initial homogeneity to approximately 80% at day 18, and further decreasing to roughly 60% at day 24.

4.2.3 Analysis of morphometric and morphological parameters of cumulus cells during culture

To assess morphological and morphometric changes in CCs over time, Phalloidin staining was performed at five time points (day 3, 8, 13, 18, and 24), covering the entire duration of the culture period [**Figure 23**], to evidence the cell boundaries.

A total of 1,309 single cells (specifically distributed as 440 cells at day 3, 272 cells at day 8, 182 cells at day 13, 129 cells at day 18, and 286 cells at day 24) were analysed utilizing the "gastruloid_morphology" algorithm (Rebuzzini et al., 2024). This automated approach enabled the precise segmentation of Phalloidin-stained cell profiles and the subsequent extraction of robust morphometric (area and perimeter) and morphological (circularity, elongation and eccentricity) parameters, revealing distinct structural shifts in the cell population over time.

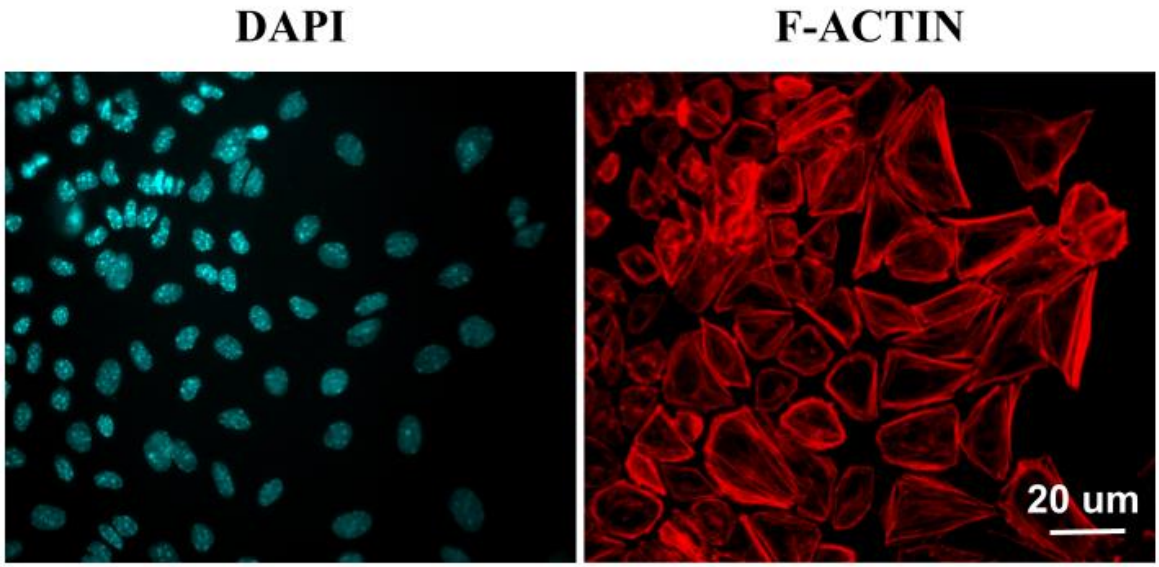

Figure 23 Representative example of cell morphology assessed by Phalloidin (F-actin, red) and DAPI (nuclei, cyan) staining at day 3 of culture

The distribution of morphometric parameters is graphically represented in the [**Figure 24]**. Regarding the cellular perimeter [**Figure 24A**], the analysis revealed statistically significant differences between all consecutive time points (*$p < 0.05$). Specifically, the perimeter underwent an initial significant increase from day 3 to day 8. This was followed by a sharp decrease at day 13, where the parameter reached its lowest values. From this point onward, a progressive and continuous increase was observed at day 18, culminating at day 24, which displayed the highest perimeter values and a broader vertical distribution. A highly significant difference was also confirmed between the initial and final time points (3 vs 24 days; ***$p < 0.001$).

Instead, cellular area [**Figure 24B**] exhibited an almost identical trend. It showed statistically significant modifications between all consecutive time points, characterized by an initial expansion in cell size at day 8, a subsequent contraction at day 13, and a final, progressive enlargement through day 18 up to day 24. In this case, a less marked but still statistical difference (*$p < 0.05$) was confirmed between day 3 and 24.

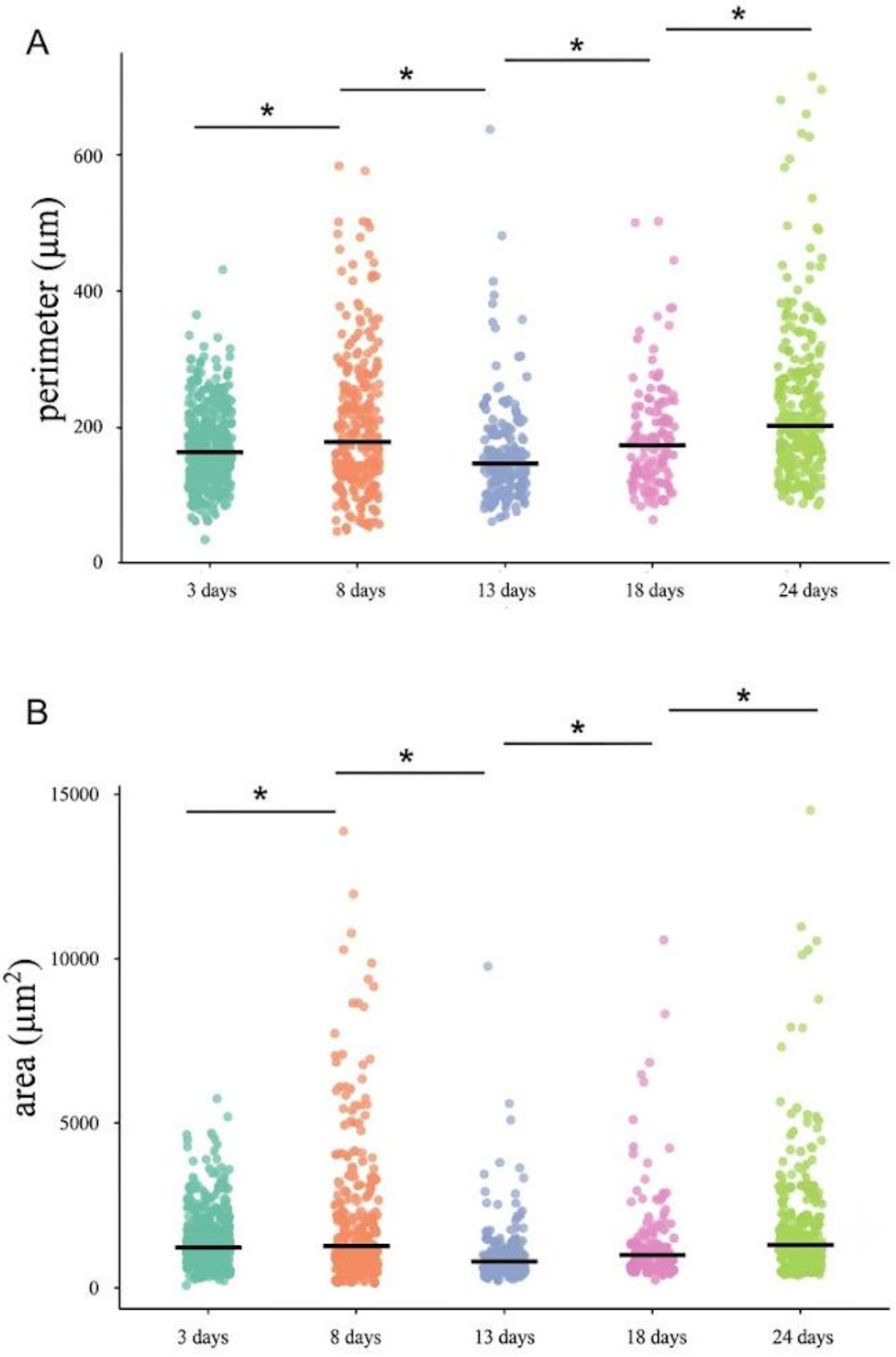

*Figure 24 Graphical representation of the distribution of morphometric parameters: A) perimeter (µm) and B) area (µm²) at day 3, 8, 13, 18, and 24 of culture, with relative statistical significance. *p < 0.05 and ***p < 0.001*

Morphological parameters modifications of the cell population over time are reported and summarized in **Figure 25**.

Regarding cellular circularity [**Figure 25A**], the analysis outlined a highly significant and progressive decline in this parameter across almost the entire culture timeline. Specifically, circularity values dropped sharply between the earliest consecutive time points, showing highly significant decreases from day 3 to day 8 (***$p < 0.001$) and further down to day 13 (***$p < 0.001$). After a brief phase of stabilization between day 13 and day 18, where no significant variations were detected, a final significant drop was recorded at day 24 (***$p < 0.001$). This overall decline trend reflects a strong shift from a predominantly round morphology at the beginning of the culture toward a highly irregular shape at the later stages, as further confirmed by the stark difference between day 3 and day 24 (***$p < 0.001$).

Cellular elongation [**Figure 25B**] followed an inverse, rising trend, indicating that the loss of circularity was directly coupled with a progressive stretching of the cell body. The elongation index showed a statistically significant increase during the first week of culture (3 vs 8 days; *$p < 0.05$), followed by a stationary plateau phase during the intermediate stages (days 8 to 18) where the values remained almost unchanged. A final, significant rise in elongation was then observed at the latest time point, between day 18 and day 24 (*$p < 0.05$), marking a definitive transition toward an elongated phenotype at the end of the culture period (3 vs 24 days; *p < 0.05).

An uniform behaviour was observed for cellular eccentricity [**Figure 25C**], a parameter that measures the deviation of the cell shape from a perfect circle. Eccentricity experienced a single significant increase at the very beginning of the experimental timeline, precisely between day 3 and day 8 (*$p < 0.05$). Beyond this initial phase, the parameter stabilized, showing no significant fluctuations among the remaining consecutive time points, although maintaining a statistically higher baseline at day 24 compared to day 3 (*$p < 0.05$).

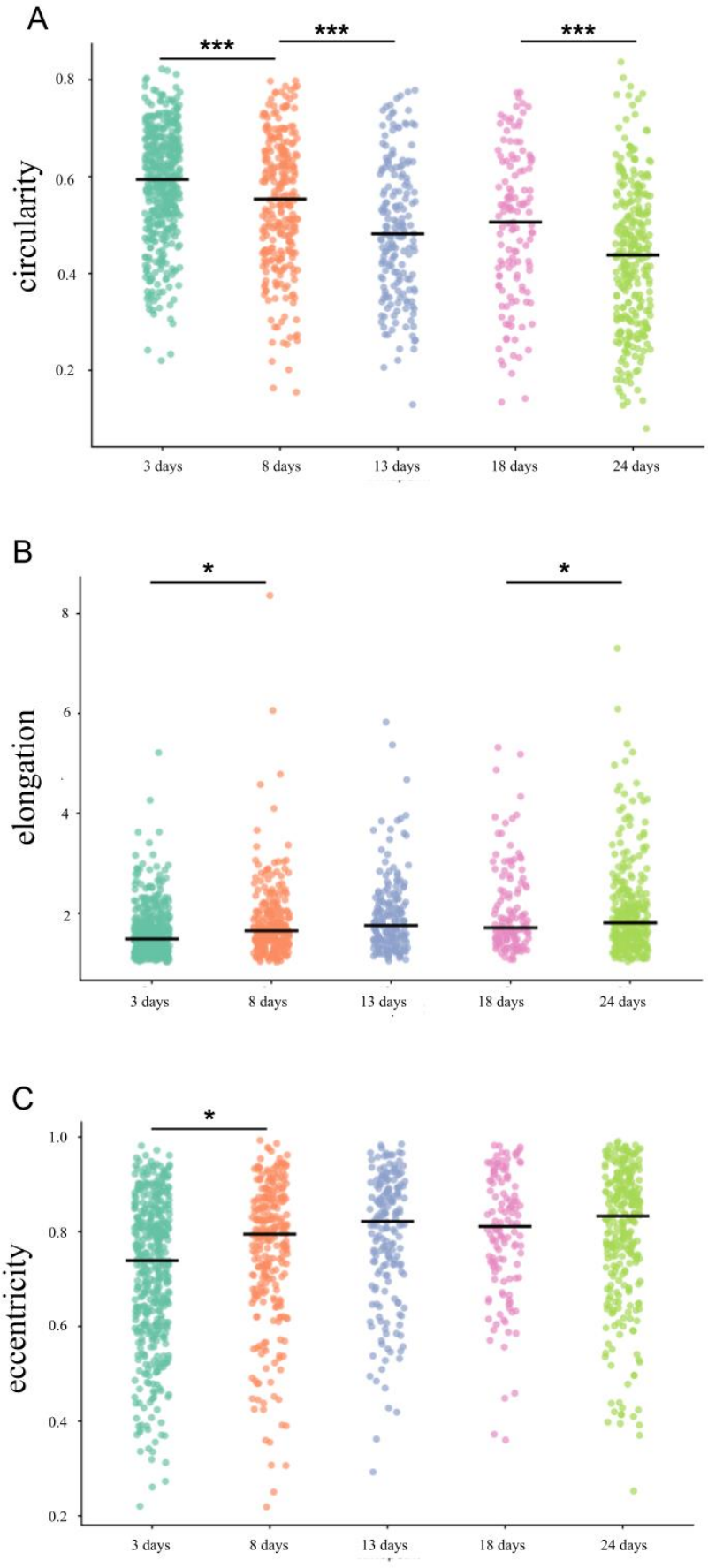

*Figure 25 Graphical representation of the distribution of morphologic parameters: A) circularity, B) elongation and C) eccentricity at day 3, 8, 13, 18, and 24 of culture, with relative statistical significance. *p < 0.05 and ***p < 0.001*

4.2.4 Gene expression analysis of Has2 and Ptx3, markers of cumulus cells

Gene expression analysis of *Has2* and *Ptx3* genes was performed, as they are key functional markers of CCs. *Has2* encodes the enzyme responsible for hyaluronic acid synthesis during cumulus expansion, while *Ptx3* encodes an essential extracellular matrix protein required for the correct organization and stabilization of the expanded cumulus matrix (Faizal et al., 2024).

Quantitative RT-PCR was performed at 3, 8, 13, 18, and 24 days during culture. The obtained results were summarized in **Figure 26**.

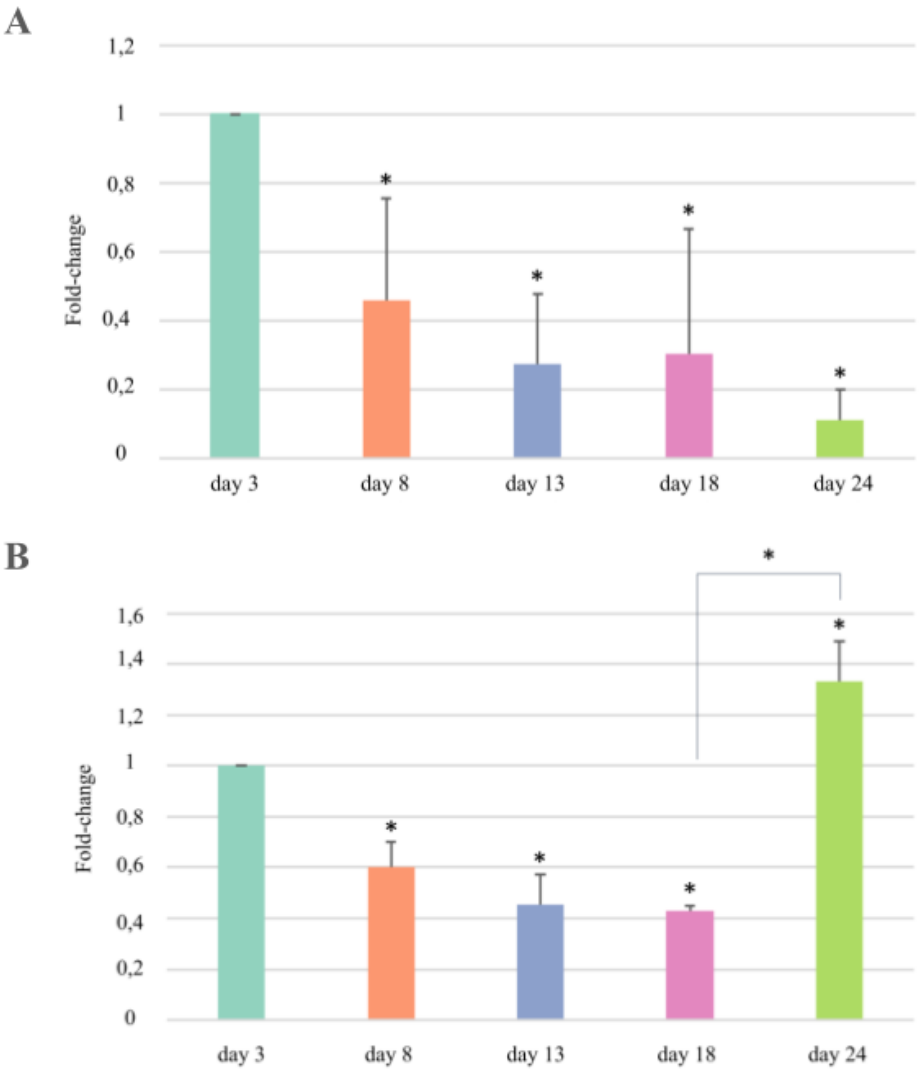

*Figure 26 Graphical representation of the expression of A) Has2 and B) Ptx3 genes. Data are expressed as fold-change relative to the expression of the genes in cells at day 3 (mean ± SD; one-way ANOVA) of culture, set at 1. The asterisks positioned directly above individual bars indicate a statistically significant difference (*p < 0.05) compared to the day 3 control. Conversely, the horizontal bracket in B, topped by the same symbol, specifies a statistically significant difference (*p < 0.05) exclusively between day 18 and day 24*

Regarding *Has2* transcriptional analysis [**Figure 26A**], the gene showed a sharp initial down-regulatio, followed by a stabilized, low-expression profile over the remaining culture period. Compared to day 3 (set as calibrator, fold-change = 1), a statistically significant reduction was already observed at day 8, with expression levels dropping to approximately 0.46 (*$p < 0.05$). Following this initial drop, Has2 mRNA levels remained low and statistically stable throughout the subsequent time points, fluctuating around 0.27 at day 13 and 0.30 at day 18, before reaching a final value of approximately 0.11 at day 24 of culture. While all time points from day 8 and further were significantly downregulated compared to the day 3 control (*$p < 0.05$), no statistically significant differences were observed among consecutive late time points, confirming that *Has2* expression quickly plateaus at a low baseline during long-term culture.

Ptx3 expression [**Figure 26B**] followed a partially similar early kinetics but exhibited a completely divergent behaviour at the late stage of culture. Transcriptional levels decreased significantly from day 3 to day 8, dropping to a fold-change of approximately 0.60 (*$p < 0.05$). Following this initial drop, Ptx3 mRNA levels reached a stationary plateau, remaining low and statistically stable at day 13 (~ 0.45) and day 18 (~ 0.43), with no significant differences detected among these intermediate time points. In severe contrast to *Has2*, however, *Ptx3* expression experienced a significant upregulation at day 24, sharply rising to a fold-change of approximately 1.33. This late-stage surge was statistically higher compared to the preceding day 18 time point (*$p < 0.05$, indicated by the bracket) and also significantly exceeded the baseline control levels of day 3 (*$p < 0.05$).

5. Discussion

Within the ovarian follicle, oocyte development relies on a bidirectional dialogue with the surrounding somatic cells. Among these, CCs, which differentiate from GCs upon antrum formation, constitute a specialized subpopulation. *In vivo*, they remain closely associated with the oocyte inside the follicle and, following ovulation, continue to surround it to form the COC. Beyond providing structural support, these cells exert vital metabolic and functional effects on the oocyte, including the regulation of glucose and amino acid uptake, cholesterol biosynthesis, the mitigation of oxidative stress, and the modulation of meiotic arrest and resumption. *In vitro*, these cells have been successfully isolated and cultured and they represent tools for predicting oocyte developmental competence and improving the outcomes of Assisted Reproductive Technology (ART) protocols.

As the role of CCs during the folliculogenesis and the maturation of the female gamete has been clearly evidenced, as well as their potential applications *in vitro* to predict or sustain oocyte developmental competence, the main objectives of this master's thesis were 1) the identification of predictive molecular biomarkers of embryonic success; and 2) the optimization of a standardized long-term *in vitro* cumulus cells culture. The present study aimed to deepen the understanding of cumulus cell biology in the acquisition of oocyte developmental competence.

The analysis on miRNAs content of human EVs derived from the two 3 days cultures of CCs (BLASTO vs. NoBLASTO) revealed the presence of 24 differentially expressed miRNAs and that several of these are already well-characterized in the literature for their involvement in ovarian physiology. Specifically, miR-24-3p, previously identified in mouse CCs (Ma et al., 2024) and porcine embryos (Stowe et al., 2012), alongside miR-320d and miR-206, both isolated from human and porcine follicular fluid EVs, are recognized as key indicators of oocyte and embryo developmental competence (Feng et al., 2015; Machtinger et al., 2017). This competence marker profile is shared by miR-132-3p, a miRNA commonly detected in human follicular fluid (Machtinger et al., 2017). Additionally, literature data demonstrate that miR-206 and miR-382-5p, both constituents of human follicular fluid, directly correlate with successful fertilization rates (Machtinger et al., 2017; Butler et al., 2019). Lastly, let-7b-5p, which is highly expressed in human granulosa cells throughout folliculogenesis from primary to antral stages, plays a documented role in modulating cell proliferation and steroidogenesis (Nazou et al., 2024). A deeper bioinformatic investigation into these miRNAs and their respective target genes suggested that the selected 24 miRNAs are directly involved in regulating fundamental genes essential for pre-implantation embryo development, oocyte maturation, meiotic resumption, the acquisition of developmental competence, cumulus expansion, ovulation, and fertilization. Importantly, the majority of these target genes (N=104) are involved in

pre-implantation development. This finding aligns with the biological context of our sample: the isolated cells derived from ovulated COCs, a stage where CCs are at the end of their life cycle and are likely transferring their final molecular cargo to the oocyte to support proper development post-fertilization. Taken together, these results may provide evidence that the miRNA cargo within EVs actively support the acquisition of developmental competence and early embryo development, starting from the regulation of the initial steps of oocyte maturation.

These insights open up promising translational applications in ART. Deciphering specific miRNAs, that added as supplements in IVM media, could potentially enhance or rescue oocyte quality (defined as the recovery and IVM of immature eggs harvested during a retrieval cycle that would otherwise be discarded due to their inability to be fertilized). This approach could significantly benefit patients undergoing ART who experience repeated cycle failures, potentially due to CC dysfunction or a suboptimal follicular microenvironment. Providing the oocyte with these critical external inputs could overcome such developmental blocks.

As an alternative strategy to using isolated EVs, CCs could be employed as a feeder layer for oocyte maturation. While this approach has been validated in mice for up to 72 hours of culture (Cavalera et al., 2019), translating it to human clinical practice requires further optimization. Interestingly, a comparison with a parallel study on mice (Fiorentino et al., 2024) highlighted a significant evolutionary convergence between the two species: among the miRNA target genes identified, 55 are shared between humans and mice, actively controlling cumulus expansion, fertilization, pre-implantation development, and meiotic resumption. However, cultures lasting up to 3 days would not be feasible or efficient for human clinical applications, where oocytes *in vitro* maturation timeframes are different, and minimizing biomaterial waste is crucial.

Consequently, the investigating a long-term mouse CC culture model was aimed to evaluate whether CCs can be successfully maintained over an extended period (beyond 3 days) while preserving their ability to sustain oocyte maturation, thereby establishing a foundation for the potential translation of long-term cultures to human clinical applications.

Based on the obtained results, despite culture evolves over the time, significant variations were not observed until day 18, considering both LAMIN B1 expression and morphological and morphometric parameters. Even though few cells characterized by a low LAMIN B1 signal, associated with senescence (Freund et al., 2012), began to appear early, their frequency remained low, reaching approximately 10% of the total population at day 18; thus, about 80% of the cells still maintained normal LAMIN B1 expression. Conversely, a critical shift was observed by day 24, where a marked increase in the low-expressing LAMIN B1 population was accompanied by profound structural

alterations. At this late time point, cultured CCs lost their circular, well-defined architecture, assuming highly irregular, bigger and elongated shapes. This strict correlation between the downregulation of LAMIN B1 and the transition toward a flattened morphology strongly suggests that the culture is progressively entering a senescent state by day 24.

Interestingly, in addition, an abnormal population overexpressing LAMIN B1 appeared as early as day 8, but remained constant throughout the culture period. This specific phenotype might be associated with spontaneous cell transformation (Kaneshiro et al., 2023), a phenomenon frequently observed in murine cells during long-term *in vitro* culture due to their intrinsic chromosomal instability and ability to overcome Hayflick limit.

Although the morphological and structural analyses suggest that the cell culture remains stable until day 18, gene expression profiles of specific CC markers reveal significant alterations starting from the beginning of the culture. Specifically, the transcriptional levels of both *Has2* and *Ptx3* undergo a marked downregulation as early as day 8. Given that these genes serve as key functional markers of cumulus cells and are fundamentally involved in the process of cumulus expansion, this early decrease likely might reflect a cellular adaptation to the *in vitro* environment. Once isolated and placed in culture, the cells are no longer part of an actively expanding cumulus oophorus; consequently, the absence of physiological, oocyte-derived stimuli might lead to the progressive downregulation of these expansion-related markers as the cells adapt to a monolayer condition.

While Has2 is maintained further at low expression during the whole culture period, Ptx3 showed a significant increase at day 24, going above even the normal expression. This behaviour could be explained by a potential dual role of PTX3: while it serves as a well-established marker of healthy CC functionality, it has also been documented to induce cellular senescence, as demonstrated in renal tubular cells (Luo et al., 2023). If the upregulation of *Ptx3* at day 24 is indeed associated with this senescent function, it would strongly corroborate the concurrent loss of Lamin B1 and morphologic and morphometric changes observed at the same time point.

At this stage, these preliminary findings provide compelling insights but are not yet exhaustive enough to definitively determine whether CCs can be maintained in vitro while fully preserving their physiological supportive functions over extended periods. Nonetheless, it is highly promising that up to day 18 of culture, no significant population shifts were observed. This suggests that these cells may successfully retain their functional activity at least until day 18.

Future perspectives

To fully unlock the clinical potential of these findings, future perspectives will be directed toward the following experimental avenues described below.

For the Part 1 of the work:

- Co-culture of oocyte on CCs feeder-layer and supplemented IVM media with EVs derived miRNAs or to evaluate their ability to rescue oocyte, improve fertilization rates, and support early blastocyst development;

For the Part 2 of the work:

- EV cargo characterization over the time: we aimed to complete the molecular characterization of EVs isolated at different culture time points
- Functional validation via IVM assay: future experiments will investigate whether CCS maintained in long term culture retain their primary physiological ability to support the IVM of denuded oocytes

6. Bibliography

1. Assou S, Haouzi D, De Vos J, Hamamah S. Human cumulus cells as biomarkers for embryo and pregnancy outcomes. Mol Hum Reprod. 2010 Aug;16(8):531-8

2. Cavalcanti GS, Carvalho KC, Ferreira CDS, Alvarez PAC, Monteleone PAA, Baracat EC, Soares Júnior JM. Granulosa cells and follicular development: a brief review. Rev Assoc Med Bras (1992). 2023 Jun 26;69(6):e20230175

3. Cavalera F, Simovic M, Zanoni M, Merico V, Garagna S, Zuccotti M. IVM of mouse fully grown germinal vesicle oocytes upon a feeder layer of selected cumulus cells enhances their developmental competence. Reprod Fertil Dev. 2019 May;31(6):1068-1077

4. Cheng EH, Chen SU, Lee TH, Pai YP, Huang LS, Huang CC, Lee MS. Evaluation of telomere length in cumulus cells as a potential biomarker of oocyte and embryo quality. Hum Reprod. 2013 Apr;28(4):929-36

5. Coticchio G, Dal Canto M, Mignini Renzini M, Guglielmo MC, Brambillasca F, Turchi D, Novara PV, Fadini R. Oocyte maturation: gamete-somatic cells interactions, meiotic resumption, cytoskeletal dynamics and cytoplasmic reorganization. Hum Reprod Update. 2015 Jul-Aug;21(4):427-54

6. da Silveira JC, de Ávila ACFCM, Garrett HL, Bruemmer JE, Winger QA, Bouma GJ. Cell-secreted vesicles containing microRNAs as regulators of gamete maturation. J Endocrinol. 2018 Jan;236(1):R15-R27

7. De La Fuente R. Chromatin modifications in the germinal vesicle (GV) of mammalian oocytes. Dev Biol. 2006 Apr 1;292(1):1-12

8. Dumesic DA, Meldrum DR, Katz-Jaffe MG, Krisher RL, Schoolcraft WB. Oocyte environment: follicular fluid and cumulus cells are critical for oocyte health. Fertil Steril. 2015 Feb;103(2):303-16

9. Eppig JJ. Oocyte control of ovarian follicular development and function in mammals. Reproduction. 2001 Dec;122(6):829-38

10. Eppig JJ. The relationship between cumulus cell-oocyte coupling, oocyte meiotic maturation, and cumulus expansion. Dev Biol. 1982 Jan;89(1):268-72

11. Esposito R, Piscopo F, Del Prete C, Kosior MA, Benedetti C, Schreiber M, Capra E, Lange-Consiglio A, Frigerio R, Lazzari B, Hoelker M, Gasparrini B. Extracellular vesicles from the follicular fluid of competent oocytes improve blastocyst yields when supplemented during simulated physiological oocyte maturation in cattle. Theriogenology. 2026 Jan 1;249:117629

12. Erickson GF,. Follicle growth and development. *Glob. libr. women's med*. 2008; doi: 10.3843/GLOWM.10289

13. Ezz MA, Balboula AZ. Molecular mechanisms of folliculogenesis and oogenesis. Syst Biol Reprod Med. 2026 Dec;72(1):211-240

14. Feuerstein P, Cadoret V, Dalbies-Tran R, Guerif F, Bidault R, Royere D. Gene expression in human cumulus cells: one approach to oocyte competence. Hum Reprod. 2007 Dec;22(12):3069-77

15. Fiorentino G, Merico V, Zanoni M, Comincini S, Sproviero D, Garofalo M, Gagliardi S, Cereda C, Lin CJ, Innocenti F, Taggi M, Vaiarelli A, Ubaldi FM, Rienzi L, Cimadomo D,

Garagna S, Zuccotti M. Extracellular vesicles secreted by cumulus cells contain microRNAs that are potential regulatory factors of mouse oocyte developmental competence. Mol Hum Reprod. 2024 May 30;30(6):gaae019

16. Freund A, Laberge RM, Demaria M, Campisi J. Lamin B1 loss is a senescence-associated biomarker. Mol Biol Cell. 2012 Jun;23(11):2066-75

17. Gilchrist RB, Lane M, Thompson JG. Oocyte-secreted factors: regulators of cumulus cell function and oocyte quality. Hum Reprod Update. 2008 Mar-Apr;14(2):159-77

18. Gilchrist RB, Ritter LJ, Armstrong DT. Oocyte-somatic cell interactions during follicle development in mammals. Anim Reprod Sci. 2004 Jul;82-83:431-46

19. Gougeon A. *Regulation of ovarian follicular development in primates: facts and hypotheses*. Endocrine Reviews. 1996 Apr;17(2), 121-155

20. Griffin J, Emery BR, Huang I, Peterson CM, Carrell DT. Comparative analysis of follicle morphology and oocyte diameter in four mammalian species (mouse, hamster, pig, and human). J Exp Clin Assist Reprod. 2006 Mar 1;3:2

21. Gruenbaum Y, Foisner R. Lamins: nuclear intermediate filament proteins with fundamental functions in nuclear mechanics and genome regulation. Annu Rev Biochem. 2015;84:131-64

22. Jurema MW, Nogueira D. In vitro maturation of human oocytes for assisted reproduction. Fertil Steril. 2006 Nov;86(5):1277-91

23. Kaneshiro JM, Capitanio JS, Hetzer MW. Lamin B1 overexpression alters chromatin organization and gene expression. Nucleus. 2023 Dec;14(1):2202548

24. Kim YJ, Ku SY, Kim YY, Liu HC, Chi SW, Kim SH, Choi YM, Kim JG, Moon SY. MicroRNAs transfected into granulosa cells may regulate oocyte meiotic competence during in vitro maturation of mouse follicles. Hum Reprod. 2013 Nov;28(11):3050-61

25. Li R, Albertini DF. The road to maturation: somatic cell interaction and self-organization of the mammalian oocyte. Nat Rev Mol Cell Biol. 2013 Mar;14(3):141-52

26. Magoffin DA. Ovarian theca cell. Int J Biochem Cell Biol. 2005 Jul;37(7):1344-9

27. Martinez CA, Rizos D, Rodriguez-Martinez H, Funahashi H. Oocyte-cumulus cells crosstalk: New comparative insights. Theriogenology. 2023 Jul 15;205:87-93

28. Massoud G, Spann M, Vaught KC, Das S, Dow M, Cochran R, Baker V, Segars J, Singh B. Biomarkers Assessing the Role of Cumulus Cells on IVF Outcomes: A Systematic Review. J Assist Reprod Genet. 2024 Feb;41(2):253-275

29. Monniaux D. Driving folliculogenesis by the oocyte-somatic cell dialog: Lessons from genetic models. Theriogenology. 2016 Jul 1;86(1):41-53

30. Nikoloff N. The key role of cumulus cells in oocytes in vitro maturation protocols. Fertil Steril. 2021 Dec;116(6):1663

31. Nilsson S, Mäkelä S, Treuter E, Tujague M, Thomsen J, Andersson G, Enmark E, Pettersson K, Warner M, Gustafsson JA. Mechanisms of estrogen action. Physiol Rev. 2001 Oct;81(4):1535-65

32. Norman AW, Henry HL. Chapter 13 - Estrogens and Progestins. In: Norman AW, Henry HL, editors. Hormones (Third Edition). Academic Press; 2015. p. 275-296. ISBN 9780123694447.

33. Ozturk S. Prediction of high-quality human oocytes and embryos through the analysis of gene expression in cumulus cells. J Ovarian Res. 2025 Dec 13;19(1):20

34. Pangas SA, Rajkovic A. Follicular Development: Mouse, Sheep, and Human Models. In *The Female Reproductive System*. Academic Press; 2015. p. 947–995.

35. Pedersen T, Peters H. Proposal for a classification of oocytes and follicles in the mouse ovary. J Reprod Fertil. 1968 Dec;17(3):555-7

36. Pedersen T. *Follicle kinetics in the ovary of the immature mouse*. Acta Endocrinologica, 1970 Jun;64(2), 304-323

37. Pietroforte S, Amargant F. Biophysical, cellular, and mouse model approaches to investigate the mechanical regulation of folliculogenesis. Semin Cell Dev Biol. 2025 Oct;174:103649

38. Rebuzzini P, Rustichelli S, Fassina L, Canobbio I, Zuccotti M, Garagna S. BPA Exposure Affects Mouse Gastruloids Axial Elongation by Perturbing the Wnt/β-Catenin Pathway. Int J Mol Sci. 2024 Jul 19;25(14):7924

39. Richani D, Dunning KR, Thompson JG, Gilchrist RB. Metabolic co-dependence of the oocyte and cumulus cells: essential role in determining oocyte developmental competence. Hum Reprod Update. 2021 Jan 4;27(1):27-47

40. Sanchez F, Le AH, Ho VNA, Romero S, Van Ranst H, De Vos M, Gilchrist RB, Ho TM, Vuong LN, Smitz J. Biphasic in vitro maturation (CAPA-IVM) specifically improves the developmental capacity of oocytes from small antral follicles. J Assist Reprod Genet. 2019 Oct;36(10):2135-2144

41. Sánchez F, Smitz J. Molecular control of oogenesis. Biochim Biophys Acta. 2012 Dec;1822(12):1896-912

42. Santonocito M, Vento M, Guglielmino MR, Battaglia R, Wahlgren J, Ragusa M, Barbagallo D, Borzì P, Rizzari S, Maugeri M, Scollo P, Tatone C, Valadi H, Purrello M, Di Pietro C. Molecular characterization of exosomes and their microRNA cargo in human follicular fluid: bioinformatic analysis reveals that exosomal microRNAs control pathways involved in follicular maturation. Fertil Steril. 2014 Dec;102(6):1751-61.e1

43. Scalici E, Traver S, Mullet T, Molinari N, Ferrières A, Brunet C, Belloc S, Hamamah S. Circulating microRNAs in follicular fluid, powerful tools to explore in vitro fertilization process. Sci Rep. 2016 Apr 22;6:24976

44. Sudewo Y, Halim B, Novi D, Adenin I, Salim Siregar H, Fidel Ganis Siregar M, Natadisastra M, Yaznil MR, Lamtota Lumbanraja I. The Role of Cumulus Cells for The Immature Oocyte Undergoing In Vitro Maturation Rescue: A Retrospective Analysis. Int J Fertil Steril. 2025 Mar 11;19(2):230-235

45. Su YQ, Sugiura K, Eppig JJ. Mouse oocyte control of granulosa cell development and function: paracrine regulation of cumulus cell metabolism. Semin Reprod Med. 2009 Jan;27(1):32-42

46. Sutcliffe MD, Tan PM, Fernandez-Perez A, Nam YJ, Munshi NV, Saucerman JJ. High content analysis identifies unique morphological features of reprogrammed cardiomyocytes. Sci Rep. 2018 Jan 19;8(1):1258

47. Tastsoglou S, Skoufos G, Miliotis M, Karagkouni D, Koutsoukos I, Karavangeli A, Kardaras FS, Hatzigeorgiou AG. DIANA-miRPath v4.0: expanding target-based miRNA functional analysis in cell-type and tissue contexts. Nucleic Acids Res. 2023 Jul 5;51(W1):W154-W159

48. Uyar A, Torrealday S, Seli E. Cumulus and granulosa cell markers of oocyte and embryo quality. Fertil Steril. 2013 Mar 15;99(4):979-97

49. Voros C, Athanasiou D, Mavrogianni D, Varthaliti A, Bananis K, Athanasiou A, Athanasiou A, Papadimas G, Gkirgkinoudis A, Papapanagiotou I, Migklis K, Vaitsis D, Koulakmanidis AM, Mazis Kourakos D, Ivanidou S, Daskalaki MA, Theodora M, Antsaklis P, Loutradis D, Daskalakis G. Exosomal Communication Between Cumulus-Oocyte Complexes and Granulosa Cells: A New Molecular Axis for Oocyte Competence in Human-Assisted Reproduction. Int J Mol Sci. 2025 Jun 3;26(11):5363

50. Weatherall E, Willmott GR. Applications of tunable resistive pulse sensing. Analyst. 2015 May 21;140(10):3318-34

51. Webb R, Nicholas B, Gong JG, Campbell BK, Gutierrez CG, Garverick HA, Armstrong DG. Mechanisms regulating follicular development and selection of the dominant follicle. Reprod Suppl. 2003;61:71-90.

52. Wigglesworth K, Lee KB, O'Brien MJ, Peng J, Matzuk MM, Eppig JJ. Bidirectional communication between oocytes and ovarian follicular somatic cells is required for meiotic arrest of mammalian oocytes. Proc Natl Acad Sci U S A. 2013 Sep 24;110(39):E3723-9

53. Zeleznik AJ. The physiology of follicle selection. Reprod Biol Endocrinol. 2004 Jun 16;2:31

54. Zeleznik AJ, Stouffer RL. Follicular Development: Mouse, Sheep, and Human Models. In T. M. Plant & A. J. Zeleznik (Eds.), *Knobil and Neill's Physiology of Reproduction*. 4th ed. Vol. 1. Elsevier Academic Press; 2015. p. 913–950

55. Zhang H, Liu K. Cellular and molecular regulation of the activation of mammalian primordial follicles: somatic cells initiate follicle activation in adulthood. Hum Reprod Update. 2015 Nov-Dec;21(6):779-86

56. Zhao Z, Sun Y, Guo R, Liang J, Dai W, Jiang Y, Yu Y, Yu Y, He L, Li D. Extracellular vesicles: Roles in oocytes and emerging therapeutic opportunities. Chin Med J (Engl). 2025 May 5;138(9):1050-1060

57. Zuccotti M, Bellone M, Longo F, Redi CA, Garagna S. Fully-mature antral mouse oocytes are transcriptionally silent but their heterochromatin maintains a transcriptional permissive histone acetylation profile. J Assist Reprod Genet. 2011 Dec;28(12):1193-6

58. Zuccotti M, Piccinelli A, Giorgi Rossi P, Garagna S, Redi CA. Chromatin organization during mouse oocyte growth. Mol Reprod Dev. 1995 Aug;41(4):479-85